CHAPTER 4

POPULATION MODELS OF AERIAL RAMETS IN *SCIRPUS GROSSUS* L.

4.1.1 Population models, plant growth, productivity and functional ecology

Plant architecture, often described as the dynamic organization of plant components and their three-dimensional (3-D) distribution, play a pivotal role in gathering multiple resources from the environment. It is those components and their spatial and time-mediated dynamics that contributed to the overall organizational architecture of a plant. For example, plant roots extend into different soil layers and adjust their direction of growth in order to take up soil water and nutrients (e.g. nitrogen, phosphorus), many of which have heterogeneous spatial distribution. Simultaneously, the acquired assimilates; water and nutrients are transported and allocated to the whole plant for growth and maintenance, expansion of existing organs and initiation of new organs. Plant architecture and their constituting components, in turn, are modified through ensuing growth and the allocation of assimilates (Fourcaud *et al.* 2008). The plant 3-D structure is then a key factor for integrating and understanding the relationships between the functions of different organs at the whole-plant level. This is the reason why describing, analyzing, modelling and simulating plant architecture has become important in the understanding the intricacy of structural demography and functional ecology of plants. The first 3-D computer simulation models of plant architecture were developed in the 1980s by Reffye and his collaborators (Reffye *et al.* 1988). With the improvement of computer capabilities, more accurate models and simulations of spatial structures of herbaceous plants and trees were developed subsequently (Prusinkiewicz and Lindenmayer 1990). However, no plant operational processes were embedded in these pioneer models, which limited their potential applications in agronomy, horticulture and forestry. To overcome this drawback, great efforts have been made from the mid-1990s

onwards to develop functional-structural (FS) plant models by combining physical and/or physiological processes (photosynthesis, assimilate partitioning, etc.) with explicit descriptions of plant structure (Perttunen *et al.* 1996; Godin and Sinoquet 2005; Fourcaud *et al.* 2008; Vos *et al.* 2010). Since then, an increasing number of researchers throughout the world has ventured into plant growth and architectural modelling and applications (Hu and Jaeger 2003; Fourcaud and Zhang 2008; Li *et al.* 2010).

The term "model" has various meanings in life sciences, depending on the target organism, temporal and spatial scales, or end users. Le *et al.* (1998) reviewed the history of plant nutrition modelling, and their application in strategic and tactical crop management, and used it as a practical tool for crop management, e.g. fertilizer recommendation. In another study Yan *et al.* (2011) showed models and simulation platforms developed in this field of research, opening brand new features to a wider community of researchers and end users. Brand new modelling technologies relating to the structure and function of plant shoots and root systems have emerged exploring from the cellular to the whole-plant and plant-community levels, generating useful data on functional-structural ecology of plants.

The architecture of plants are affected by endogenous factors such as hormone signals and trophic competition between organs (often described as integration of modules [*sensu* Baki 1986]), but also by exogenous factors such as light distribution, temperature, soil water and nutrient regimes. Thus, plant morphology can as well be artificially modified, at least theoretically. Many efforts have been made in the last decade to model the structural development of plants taking into account their plasticity, which is their ability to adapt their shape and to regulate their functions in a changing environment (Yan *et al.* 2011). This is illustrated by the work of Pallas *et al.* (2011) who investigated the architectural growth of grapevine (*Vitis vinifera*). Cieslak *et al.*

(2011) developed an L-system based model of a kiwifruit vine that integrates structural development, carbon dynamics, and environmental and management effects on vegetative and generative components. Jullien *et al.* (2011) evaluated the costs of ramification through quantifying the interaction between architecture and source-sink dynamics in the winter crop and oilseed rape (*Brassica napus*). This work provides promising clues for the construction of functional–structural plant models for plants with complex architectural plasticity and oleaginous components.

It is important to quantify the growth and development of plants and their interaction with fragile ecosystems. For example, the morphology of rice (*Oryza sativa*) has been substantially modified by breeding in recent decades in order to enhance its yield potential. In this context, genetic analyses of morphological traits have been investigated in detail (Yang and Hwa 2008; Qian *et al.* 2011). An functional-structural plant model of rice was developed by Xu *et al.* (2011), which allows computation of various phenotypes as a result of basic eco-physiological processes (Xu *et al.* 2011). In another study included the biomass, plant height, crown diameter, flower number and days of blooming of *Begonia xelatior* under the effect of different watering frequencies and fertilizer amounts. The results of main factor analysis indicated the effect of the fertilizer amount was greater than that of watering frequency, and the amount of water being added and fertilizer amount matching the optimal indexes was conducted as well. The effects of water and fertilizer on the growth index and quality indexes of *B. xelatior* was obtained by single factor analysis (Sun and Zhang 2011). Similar studies were done on the biomass of *Lactuca sativa* under the effects of K, P, N fertilizer and water (Yan *et al.* 2011),.

4.1.2 Fractals and fractal dimensions

Fractals are widely used by geologists to model correctly the behaviour of a wide set of natural phenomena and, in particular, to characterize the geomorphology of natural surfaces (Turcotte 1997). Within this framework, the fractal dimension is a concise and meaningful parameter with solid mathematical and physical background bearing crucial information for the geophysical characterization of the surface (Mandelbrot 1983; Turcotte 1997).

Fractal dimension is an interesting parameter to characterize roughness in an image. It can be used in texture segmentation, estimation of three-dimensional (3D) shape and other information (Sarkar and Chaudhuri 1992). This analysis has received increasing attention as a number of studies have shown fractal based measures to be useful for characterising complex biological structures. Fractal scaling is evident in natural objects from the micro- scale to the macro-scale (Corben 2001), and has been used to investigate weeds and corn crops. Using Excess Green minus Excess Red (ExG − ExR), coloured vegetation can be separated from the various field backgrounds, and the corresponding gray level images with a uniform background are acquired (Wu *et al.* 2009).

4.1.3 Response surface analysis

The response Surface Analyses is a method for studying geometric relations among responses generated by a mathematical model that is often used in nonlinear regression (Bates and Watts 1988). For a model with p parameters and n observations, the response surface is defined as a p-dimensional surface formed by all promising response vectors that the model can describe. The response surface is embedded in the n-dimensional data space, which is the set of all promising response vectors that could be generated

independently of any model. The response surface is a hyper plane for a linear model but may be curved when the model is nonlinear (Myung 2000). Many statistical concepts, including those of least square's estimation, have informative geometric interpretations in terms of response surfaces. In particular, effect of averaging on model fit can be seen quite clearly when averaged and individual data are plotted in the space of response surfaces (Myung 2000).

4.1.4 Objectives of study

In this study, assessment of growth of above-ground plant populations of *S. grossus*, and architectural models of displayed by and measured through emergence of ramets and plants height grown under different soils and fertilizer regimes are developed. In addition fractal analysis and fractal dimensions of time-based emergence of ramets and their heights are carried out.

MATERIALS AND METHODS

4.2.1 Growth patterns and population models of ramets of *Scirpus grossus* in peat soil

Synthetic populations of *S. grossus* were established on peat soils in the Malaysian Agriculture Research Development Institute (MARDI) Research Station, Jalan Kebun, Klang (N 2.98^{o} / E 101.50^{o}), Malaysia for 24 weeks commencing on 24 February 2010. Young ramets at 2-3-leaf stage of *S. grossus* were obtained from rice fields of Tanjung Karang, Selangor. Each ramet was planted in the centre of a plot measuring 2 m x 2 m, previously demarcated and lined with 5 cm x 5 cm grids and sub-plots. The details of

experimental layout, plant care and population census and data recordings are shown in Chapter 2 (pp. 80 - 101).

The mean rainfall and temperature data are shown in Fig. 2.5 (p. 69), while the physio-chemical characteristics of peat soils are shown in Table 2.9 (p. 141).

4.2.2 Growth patterns and population models of ramets of *Scirpus grossus* in paddy soil

Synthetic populations of *S. grossus* were established on paddy soils in the Malaysian Agriculture Research Development Institute (MARDI) Research Station, Tanjung Karang, Selangor (N 3.28^{o} / E 101.08^{o}), Malaysia for 24 weeks commencing on 26 October 2010. The procedures of planting and plant care of *S. grossus* during experimentation were similar to the earlier experiment on peat. Please refer to pp. 63 - 67 for details on experimental layout, plant care and population census and data recordings are shown in Chapter 2 (pp. 80 - 101). The mean rainfall and temperature data are shown in Fig. 2.6 (p. 72), while the physio-chemical characteristics of peat soils are shown in Table 2.9 (p. 144).

4.2.3 Data recording and collation

Table 4.1 enlists the full data collected in this experiment and the type of statistical treatments accorded for peat soils, while Table 4.2 enlists the full data collected in this experiment and the type of statistical treatments accorded for paddy soils.

4.2.3.1 Patterns of ramets emergence

The ramets number was determined by counting the number of ramet/plant on a weekly basis. For each plot all ramet growth parameters, namely height, number, and time of emergence for each treatment were recorded on the map.

4.2.3.2 Ramets dynamics

Ramet fluxes including gross, mortality and net number were assessed by counting the number of ramet/plant on a weekly basis. For each plot all emerged ramet were selected for measurement for each treatment and recorded on the map. The mortality number equals to the number of dead plants.

4.2.3.3 Ramets height

Ramets height was recorded from the ground to highest leaf tip, using a centimeter scale and determined on a weekly basis. For each plot, 15 ramets were randomly selected for measurements per treatment.

4.2.3.4 Dispersion analyses of *Scirpus grossus* in peat and paddy soils

The circular statistics dispersion analyses of emerged ramets in both fertilized and unfertilized paddy soils are a sub field of statistics, which is devoted to the development of statistical techniques for the use with data on an angular scale. On this scale, there is no designated zero and, in contrast to a linear scale, the designation of high and low values is arbitrary. Circular statistics is employed to look at the circular distributions of grown emerged ramets around the mother plant of *S. grossus*. This was carried out for

all replicates in both unfertilized and fertilized plots. Following this, Rayleigh's z test was conducted to test whether there is a significant mean direction in the emerged ramets with respect to the geographical north (Zar, 2006).

4.2.3.5 Fractal dimension of gray-levels

The typical technique for determination of The box-counting dimension (BCD) consists in partitioning the image space in boxes of size d x d and counting the number N(d) of boxes that contain at least one part of the shape to be investigated. Several values of d are chosen and the least square fitting of log[N(d)] x log(d) was used to determine the value of BCD. However, this approximation will suffer the effects caused by spatial quantization as well as the limited fractals of most natural objects. Therefore the curve log[N(d)] x log(d) will exhibit two distinct regions. The error was minimized calculating D in the region where the curve was most linear. Such guidelines were applied in the present research (Corben 2001).

The steps of the box-counting algorithm were as following: The original greyscale image was threshold to create a binary image, where leaves were represented by black pixels. An edge detection algorithm was applied to the binary image to create an image containing only the edge of the leaf. The edge image was divided into a grid of square sub-images, or "boxes", of fixed length, d, and the number of boxes containing part of an edge, N(d), was counted. N(d) was determined for a range of values of d, and then the log[N(d)] versus log(d) was plotted. The most linear portion of the curve was chosen and linear regression was performed on that segment of the curve. The BCD was the negative of the slope of the regression line (Corben 2001).

4.3.1 Above-ground plant population models of *Scirpus grossus*

4.3.1.1 The growth patterns of ramets in fertilized and unfertilized peat and paddy soils

This study was an attempt to determine the effects of NPK fertilizer application and soil types on the structural demography and aerial growth, including phenology of ramets in *Scirpus grossus* reiterates by rhizomatous growth and branches from a single mother plant. Irrespective of the fertilizer regimes, the sedge demonstrated a lag-phase in the recruitment of aerial modules (ramets) in the first 6 weeks after transplanting (for peat soils) or up to 8-10 weeks in the paddy soils, only to be followed by relatively faster growth rates up to 18th week for peat soils or through and through to 24th week after experimentation in paddy soils (Tables 1, 2; Fig. 44.1a, b, 4.2a, b). It was apparent that in peat soils, the sedge reached the asymptotic growth pattern in the 18 – 24 weeks period, but sedge in the paddy soils did not display the growth asymptote even after 24 weeks of experimentation. The relatively more robust growth of the sedge in the peat soils *vis-a-vis* the paddy soils may be due to easier penetration of soil lattices and bud breaks in the former soils. Paddy soils are relatively harder compared to peat soils to penetrate by the subterranean rhizomes from where aerial ramets emerged. It is difficult at this juncture to speculate whether these disparities in growth performance of the individual sedge were attributed to differences in relative availability and accessibility of nutrients in both soils. Such notion will need radio-tracer studies on the relative availability of nutrients and their relative uptake by the sedge when subjected to paddy and peat soil regimes. In both peat and paddy soils, fertilized or otherwise, there were time-mediated increments in the recruitment of ramets by the sedge, albeit differences in the number of ramet modules that emerged. As shown in Table 4.1 and Fig. 4.1, the

best period of clonal growth in general was between 10 - 16 weeks in peat soils. At the end of the 24 weeks of study period, the total average gross number of emerged ramets in fertilized soils were 126.75 ramets m^{-2} and 117.83 ramets m^{-2} in unfertilized soils, and these recruitments were not significantly different at $p<0.05$ (HSD tests). In the case of paddy soils, the parallel figures were between 8-16 weeks, where ramet recruitments displayed higher rates of emergence (Table 4.2, Fig. 4.2), albeit in lower quanta compared with their counterparts in peat soils. The best period of clonal growth in general was between 8-16 weeks. At the end of 24 weeks of study period, the total average gross number of emerged ramets in fertilized soils were 97.08 ramets m^{-2} and 83.67 ramets m^{-2} in unfertilized soils, denoting significant difference at $p<0.05$ (HSD tests).

As explained in Chapter 2, pp. 78 - 90, mortaility of emerged ramets set in Table 2.1 in fertilized peat soils and in the unfertilized peat soils. The parallel figures for paddy soils were 24 weeks after transplanting, respectively. These mortalities were to the tune of 30.33 ramets m^{-2} in unfertilized peat soils and 8.67 ramets m^{-2} in fertilized soils, leaving respective net populations of 87.5 ramets m^{-2} and 116.08 ramets m^{-2} after 24 weeks of experimentation (Chapter 2, pp. 80 - 93). In paddy soils, the total ramet mortalites were 8.58 ramets m^{-2} in unfertilized soils and 5.67 ramets m^{-2} in fertilized soils leaving respective net populations of 75.09 ramets m^{-2} in unfertilized soils and 91.41 ramets m^{-2} in fertilized soils, these populations were not significantly at $p<0.05$ (HSD tests). These findings are in agreement with those reported by Baki (1988). This phenomenon is probably due to the finite amount of a resource in the soil, which diminished with time with time. In addition to this although there may be resources still available, the plants are ageing and the leaves start to show reduced effective photosynthesis. Furthermore, the assimilatory activity of the plant may have been

approaching the compensation point with the respiratory burden of accumulated support tissue.

As with ramet recruitments, the mean plant heights of individual ramets in peat and paddy soils, fertilized or devoid of fertilizer displayed time-mediated increase (Tables 4.1, 4.2; Figs. 4.1 4.2), with lag phases in the first 6 weeks after transplanting (for peat soils) or up to 8-10 weeks in the paddy soils, only to be followed by relatively faster growth rates up to 18th week for peat soils or through and through to 24th week after experimentation in paddy soils (Tables 1, 2; Fig. 4.1a, b, 4.2a, b). The mean height of ramets in plots devoid of fertilizer application was on 93.0 cm while their counterparts in the fertilized plots reached 121.3 cm in height 16 weeks after transplanting. The ensuing increments in plant height 20 weeks onwards were fairly similar. In paddy soils, plant height of individual ramets were relatively taller than those grown in peat, with or without fertilizer applications (Tables 1, 2; Fig. 4.1a, b, 4.2a, b), reaching respective heights of 175.3 cm and 172.6 cm.

It should be noted here that in peat soils, with or without fertilizer applications the recruitments of aerial modules were more spread (likewise the sub-terranean rhizomes, extending themselves outside the designated 2 m x 2 m experimental plots). Because of this, phototropism phenomenon was not so prominent among the aerial ramets to seek more light, hence, greater height display as in the case of those ramets in the paddy soils. Ramets in paddy soils, however, grew in very tight clumps, displaying the phalanx strategy in the exploitation of space, with less space-mediated rhizomatous growth below the soils surface.

In terms of biomass accumulations of selected plant parts of *S. grossus* taken after harvest at 24 weeks after transplanting, they displayed measurable differences

according to fertilizer regimes. In unfertilized peat soils: the leaves were 6.90 g, and the stems, 7.99 g whilst the flowers were 1.92 g in weight. In fertilized peat soils these were measurably higher with 9.73 g (leaves), 10.51 g (stems) and 2.77 g for flowers (Table 3.7). The dry biomass of selected plant parts of *S. grossus* taken after harvest at 24 weeks after transplanting, showed measurable differences according to fertilizer regimes. In unfertilized paddy soils: the leaves were 12.72 g, and the stems, 17.56 g whilst the flowers were 2.38 g in weight. In fertilized paddy soils these were measurably higher with 14.84 g (leaves), 18.61 g (stems) and 3.13 g for flowers (Table 3.8) (Chapter 3, pp. 163 - 164). Invariably, fertilizer applications, albeit differential response, enhanced biomass accumulation in all plant parts of the sedge compared with those cohorts devoid of fertilizer treatments, indicating the capacity of *S. grossus* to exploit available at their disposal. Interesting despite their relatively less in number, the sedge in paddy soils were heavier compared those in peat soils, accumulating more dry matter in all plant parts, leaves, stems and inflorescence. These data perhaps explain the richer nutrient status of paddy soils, hitherto receiving fertilizers from nearby paddy plots, while the experimental in peat soils in Jalan Kebun were devoid of fertilizer applications, being uncultivated, for quite some time before experimentation. The nutrient status of peat and paddy soils are shown in Tables 3.4 (Chapter 3, pp. 180).

These results showed that the use of fertilizers had a significant impact on content in growth parameter but others did not show a significant impact. The addition of NPK fertilizer had a significant effect on clonal growth where it dramatically increased the population flux of the weed. Similarly, the NPK fertilizer caused a decrease in the number of deaths of ramets, and this was similar to the findings of Baki (1988) who studied the structural demography and growth patterns of *S. grossus.* The NPK fertilizer, which contains 30% of phosphate, also increased the flowering rate of

the weed. Baki (1988) reported similar observations. In addition, the NPK fertilizer helped to strengthen the plant and this was observed in the significant increase in the weights of the various plant parts in fertilized soils. Many previous studies have shown that the application NPK fertilizer can effect clonal growth of crop plants, such as wheat (Ognjanovic *et al.* 1994; Biberdzic *et al.* 2011). Philip *et al.* (2011) reported, in experiments that took 3 years, on the impact of different fertilizers types on the growth of potato shoots and roots, where he observed that the highest percentage yield in NPK fertilizer treated plants. NPK affected the physiological health of the plant and increased the size of the leaves. In another study, phosphate played a significant role in affecting stages of plant growth (Hatem *et al.* 2011). Agbede (2010) proved that the fertilizer caused an increase in biomass for *S. jacobaea, S. vulgaris* and *S. aquaticus* plants.

Table 4.1 Mean gross number of aerial ramets (m^{-2}) and plant height of *Scirpus. grossus* plant grown in fertilized (F1) and unfertilized (F0) peat soils at MARDI Research Station, Jalan Kebun, Selangor, Malaysia[#]

Weeks after transplanting	Gross number of ramets		Plant height (cm)	
	F0	F1	F0	F1
2	0.92 g	0.75 ij	14.00 jk	11.67 jk
4	1.67 fg	1.67 ghi	23.00 ijk	23.50 ijk
6	4.92 efg	4.42 ghi	28.00 ijk	26.83 ijk
8	10.50 defg	11.17 efgh	30.67 ijk	29.67 ijk
10	26.17 bcdef	26.75 cdefg	35.83 hij	40.67 hij
12	50.92 abcd	53.92 abcde	43.83 ghi	63.17 ghi
14	74.17 abc	81.42 abc	59.67 efg	92.33 efg
16	95.50 ab	101.67ab	93.00 cde	121.33 cde
18	105.25 a	105.67 ab	124.67 abc	143.33 abc
20	109.83 a	120.17 ab	135.00 abc	143.33 abc
22	116.83 a	125.17 a	156.33 a	153.00 a
24	117.83 a	126.75 a	161.67 a	160.67 a

[#]Figures in a column with same lowercase letters are not significantly different at $p<$ 0.05 (HSD tests).

Table 4.2 Mean gross number of aerial ramets (m^{-2}) and plant height of *S. grossus* plants grown on fertilized (F1) and unfertilized (F0) paddy soil at MARDI Research Station, Tanjung Karang, Selangor, Malaysia[#]

Weeks after transplanting	Gross number of ramets		Plant height (cm)	
	F0	F1	F0	F1
2	0.00 j	0.75 l	17.67 j	21.67 j
4	0.00 j	2.00 jk	19.67 ij	27.83 ij
6	1.00 hij	3.92 hij	27.83 hij	34.50 hij
8	2.33 fgh	6.75 fgh	34.33 ghij	48.67 ghij
10	4.92 f	10.58 f	47.67 fghi	76.00 fghi
12	15.83 e	25.83 e	67.43 efg	95.27 efg
14	34.42 cd	43.83 cd	101.67 cde	118.67 cde
16	48.00 abc	64.92 abc	120.67 bc	144.33 bc
18	54.67 abc	72.33 abc	135.83 abc	154.33 abc
20	63.92 ab	80.83 ab	142.00 abc	158.83 abc
22	74.67 ab	88.08 ab	155.33 ab	165.67 ab
24	83.67 ab	97.08 a	172.67 ab	175.33 a

[#]Figures in a column with same lowercase letters are not significantly different at $p<$ 0.05 (HSD tests).

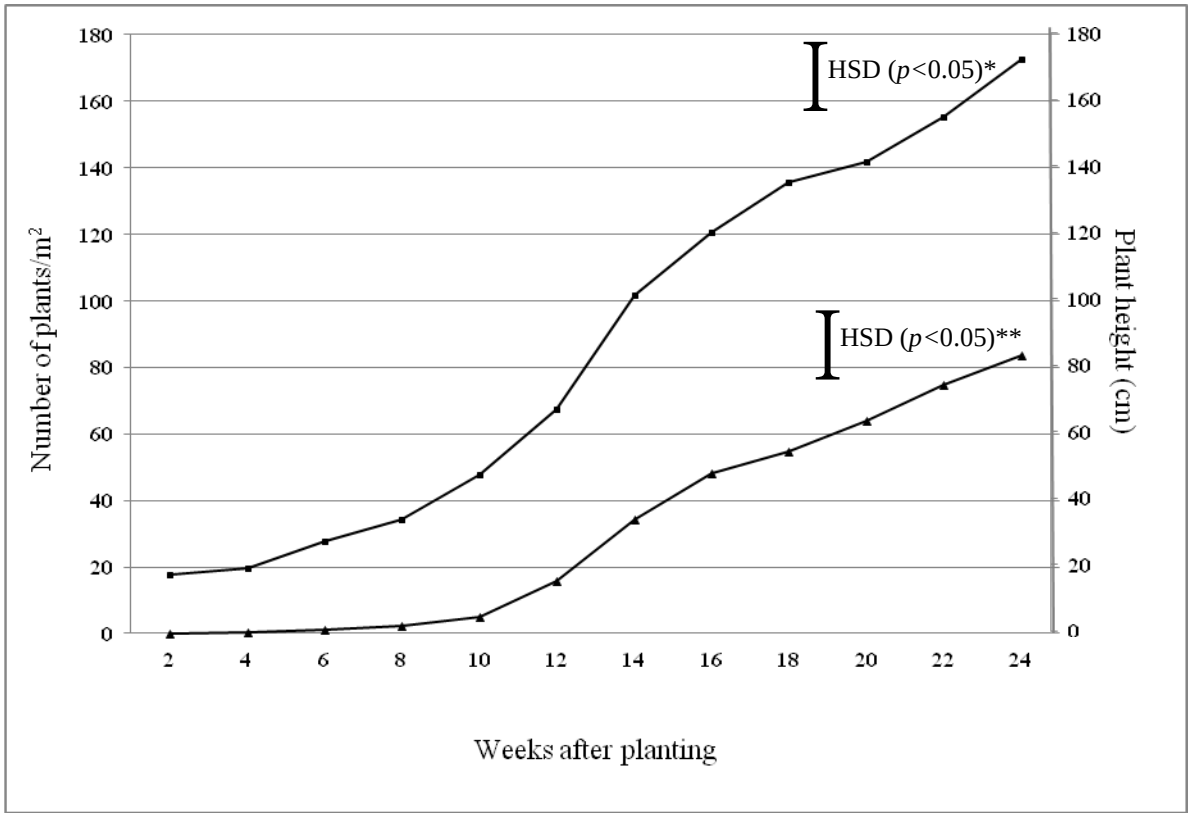

Fig. 4.1a Population increase of aerial ramets and plant height of *Scirpus grossus* grown on unfertilized (F0) peat soil. Plant number (▲), Plant height (■).*Plant number, ** Plant height.

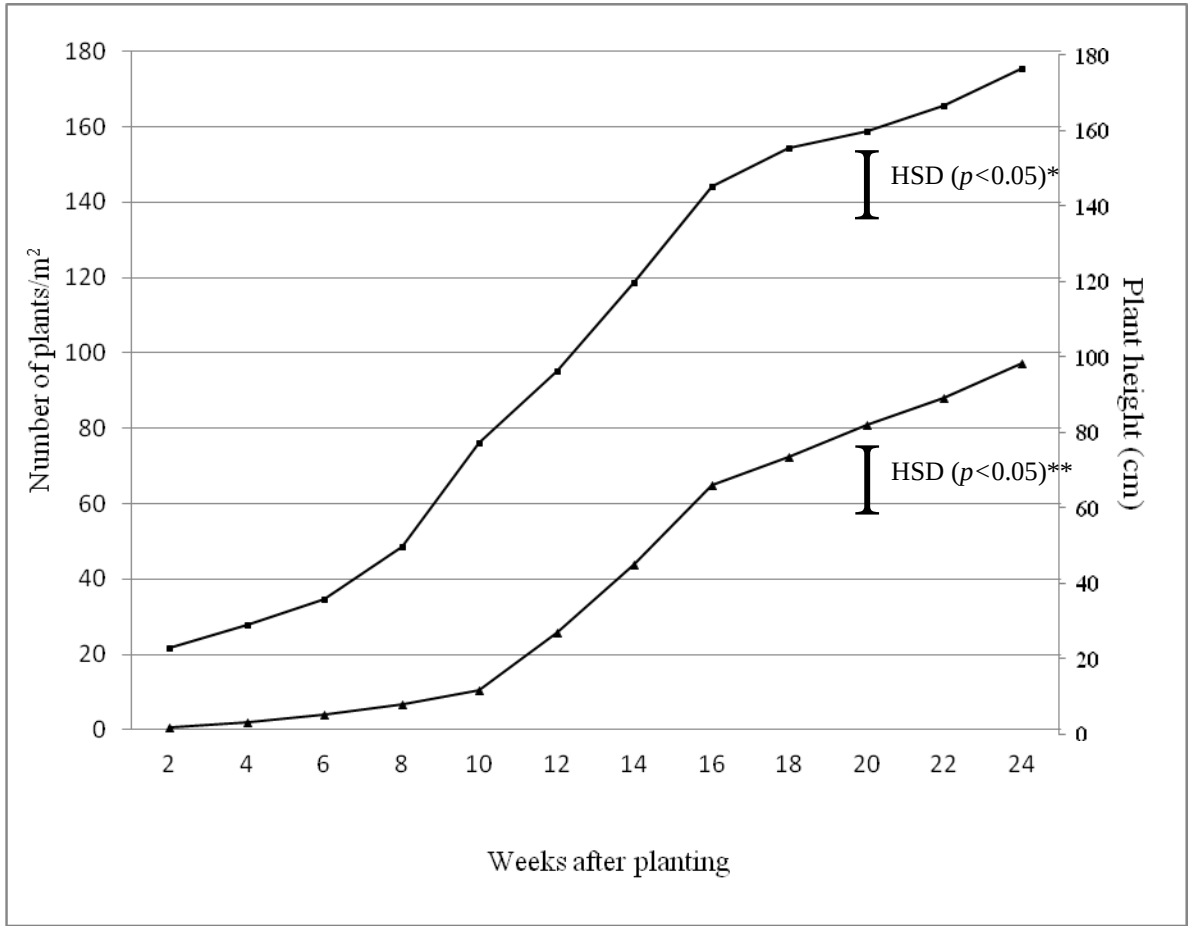

Fig. 4.1b Population increase of aerial ramets and plant height of *Scirpus grossus* grown on fertilized (F1) peat soil. Plant number (▲), Plant height (■).*Plant number, ** Plant height.

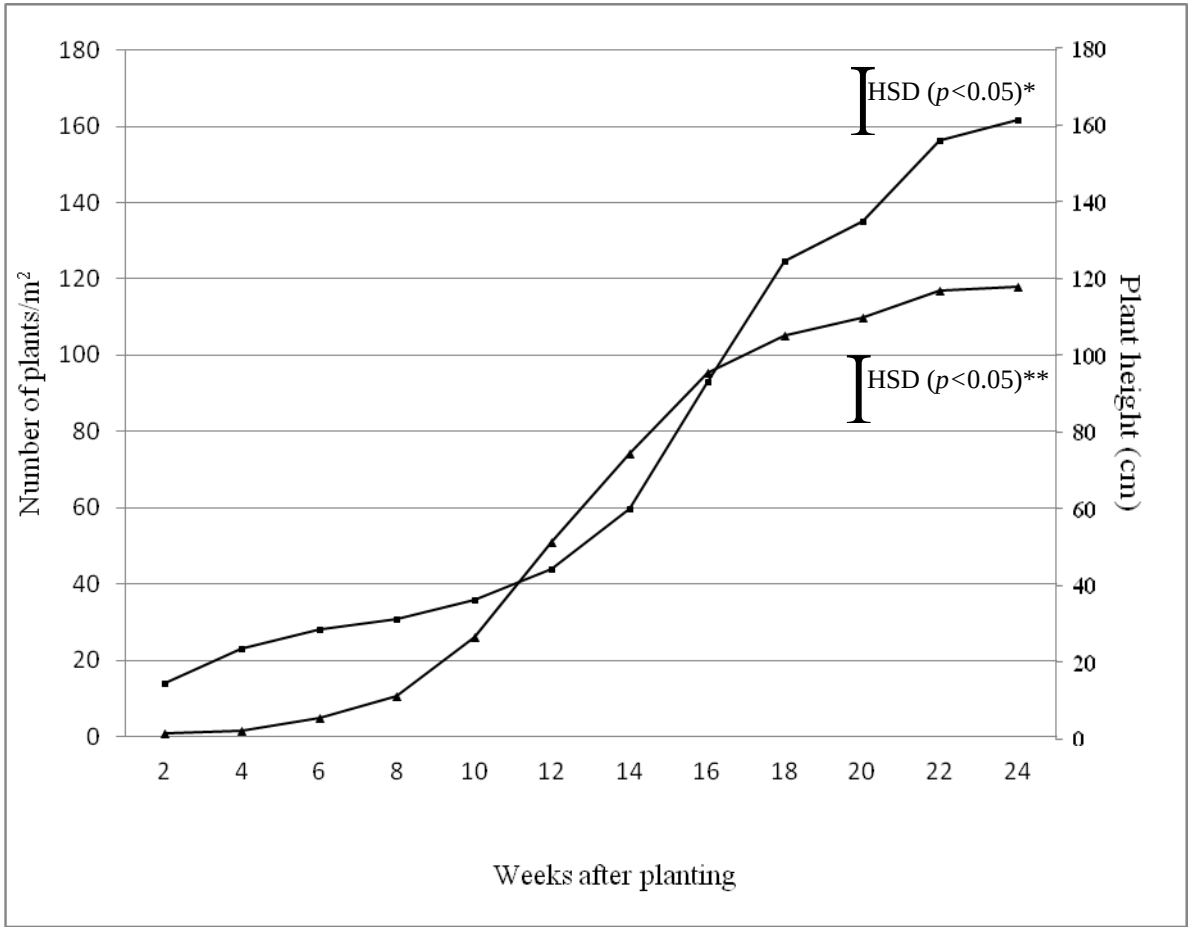

Fig. 4.2a Population increase of aerial ramets and plant height of *Scirpus grossus* grown on unfertilized (F0) paddy soil. Plant number (▲), Plant height (■).*Plant number, ** Plant height.

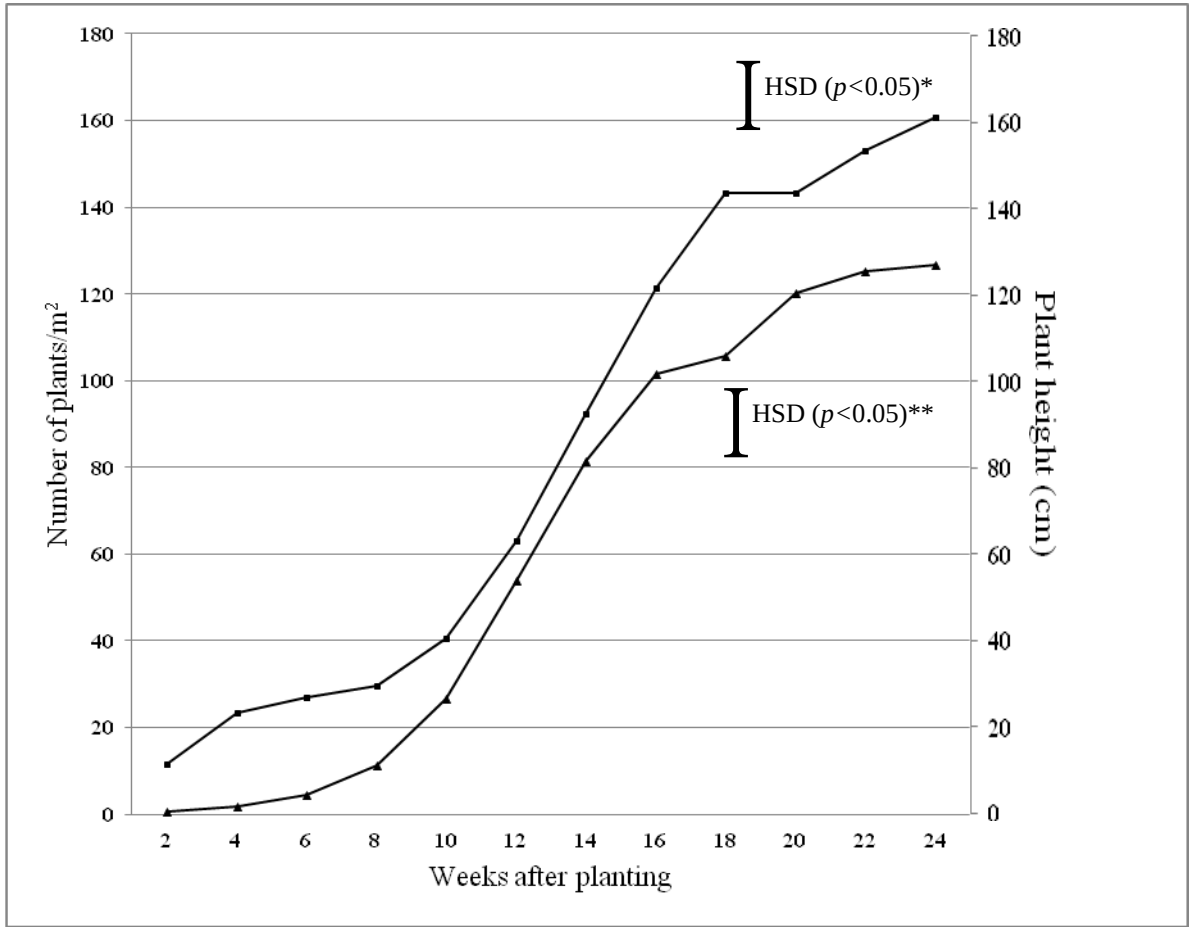

Fig. 4.2b Population increase of aerial ramets and plant height of *Scirpus grossus* grown on unfertilized (F1) paddy soil. Plant number (▲), Plant height (■).*Plant number, ** Plant height.

4.3.2 Phenology of *Scirpus grossus* grown

4.3.2.1 Phenology of *Scirpus grossus* grown in peat and paddy soils

The time-mediated flower emergence of ramets in both fertilized and unfertilized peat soils are shown in Figs. 4.3 to 4.14 Invariably, more ramets set flowers in fertilized soils than those in the unfertilized counterparts (38.75 ramets m^{-2} *vis-a-vis* 51.58 ramets m^{-2}), indicating the stimulatory effects of fertilizer application of the growth, proliferation and enhancement of flowering of *S. grossus*. The results for subsequent recruitment of shoot modules appeared convergent where the highest average plant height in unfertilized soils was 161.67 cm while in fertilized soils it was 160.67 cm, not significantly different at 0.05%.

The time-mediated flower emergence of ramets in both fertilized and unfertilized paddy soils are shown in Figs. 4.15 to 4.26 Invariably, more ramets set flowers were recorded in fertilized soils than those in the unfertilized counterparts (16.42 ramets m^{-2} *vis-a-vis* 23.67 ramets m^{-2}), indicating the stimulatory effects of fertilizer application of the growth, proliferation and enhancement of flowering of *S. grossus*. The results for subsequent recruitment of shoot modules appeared convergent where the highest average plant height in unfertilized soils was 161.67 cm while in fertilized soils it was 160.67 cm, not significantly different at 0.05%.

The results explained that most N and P to the two active role in increasing plant growth and development (Levi *et al.* 2011). Kolb *et al.* (2002) found that the exotic annual weed *Lolium multiflorum* grew at a faster rate and increased its competitive effect more than the perennial native weed *Hordeum brachyantherum*. In the presence of N, Abraham *et al.* (2009) also found the performances of exotic and native plant species with annual and perennial life histories with increased N availability and found

species-specific results. Although, P has been studied less than N have been shown to limit the growth of *B. tectorum* in the field (Miller *et al.* 2006; Gundale *et al.* 2008) and *B. tectorum* tend to invade patches of high P availability (Bashkin *et al.* 2003). Because retardant has high concentrations of both N and P. The results showed that the use of week-to-week differences had a significant impact on content in growth parameter, mortality rate, highest average plant height, weights of the various plant parts and flowering ramets.

4.3.2.2 Aerial modular growth of *Scirpus grossus* grown in peat and paddy soils

Figures 4.3 – 4.26 display the time-mediated emergence and ensuing growth of aerial modules (ramets) of *S. grossus* with or without fertilizer applications on peat and paddy soils of Jawa series. Reversing the terminology of the economic analysts, Kurosaki *et al.* (2003) "*rich periphery, poor center"* phenomenon (*sensu* Kurosaki *et al.* 2003), we can visualize the heavy loads of population pressure in the centre of the 2 m x 2 m plots among cohorts of S. *grossus.,* while in the periphery the opportunistic strategy of continuing exploitation space, and "edge effect" (*sensu* Baki 1980) prevails unabated. It is very obvious that there 6-monthly cohorts in the 6 months old plot (Fig. 4.9, 4.15, 4.21, and 4.26) with different stages of growth and perhaps with different needs for nutrients and space. These cohorts were not detached from the mother plant in the centre. The basic question arising from this juxtaposition of aerial modules, is how are nutrients being strategized to achieve optimal growth, or is there any optimal growth at all at a particular point of time and space? The fact that these cohorts are not detached but interconnected from each other, points to the arguments proposed by Baki (1986, 1988) that some kind of integration modules occurs so as to allow, more active growth

not in the centre of the 2 m x 2m plots but in the peripheral growing points for more emergence of new modules, or "*poor in the centre, rich in the periphery"* phenomenon, in a reversal way as advocated by Kurosaki *et al.* (2003). It would serve another research frontier to have radio-tracer technique studies perhaps with C^{14} to autoradiograph the nutrients pathway fed from the centre and follow through their movements.

Figures 4.3 - 4.26 display the spatial spread and proliferation of aerial modules (ramets) of *S. grossus* as the functions of time, soil types and fertilizer application. It is very obvious that albeit narrow differences that fertilizer applications and soil types influenced the nature of spread and growth of aerial modules with more modules emerged in plots grown on peat soils that their counterparts in paddy soils. Fertilizer application did have some effects in the number of aerial modules that emerged and their subsequent time-mediated proliferations.

Going through Figs. 4.3-4.8, Figs. 4.9-4.14, Figs. 4.15-4.20, and Figs. 4.21 – Fig. 26, we can see the differential growth of cohorts of the sedge mediated through time and as influenced by soil types. In fact, differences were obviously displayed in terms of mean plant heights ranging from 23.0 cm in the first month after transplanting to an array of heights (30.67 cm; 43.83 cm; 93.00 cm, 135.00 cm and 161.67 cm) in plots devoid of fertilizer application on peat soils. The parallel figures for cohorts in the fertilized plots are 23.5 cm in the first month after experimentation to 23.5 cm, 29.6cm, 121.3 cm, 143.3 and 160.67 cm. In unfertilized paddy soils, the parallel readings were 19.67 cm in the first month after transplanting from 19.67 to 172.67 cm five months later. The sedge in the fertilized paddy soils registered 27.8 cm in plant height one month after transplanting to 175.4 cm five months later. We could explore a series of regression analyses to model plant height increments and other growth parameters like

time-mediated biomass allocation as we change the variables, soil types, nutrient availability, change in soil pH, etc. Again, these serve new frontier for further research on population biology of the weed in our attempts to understand the underlying strategy for growth and survivorships of rhizomatous modular plants, in this case *S. grossus*.

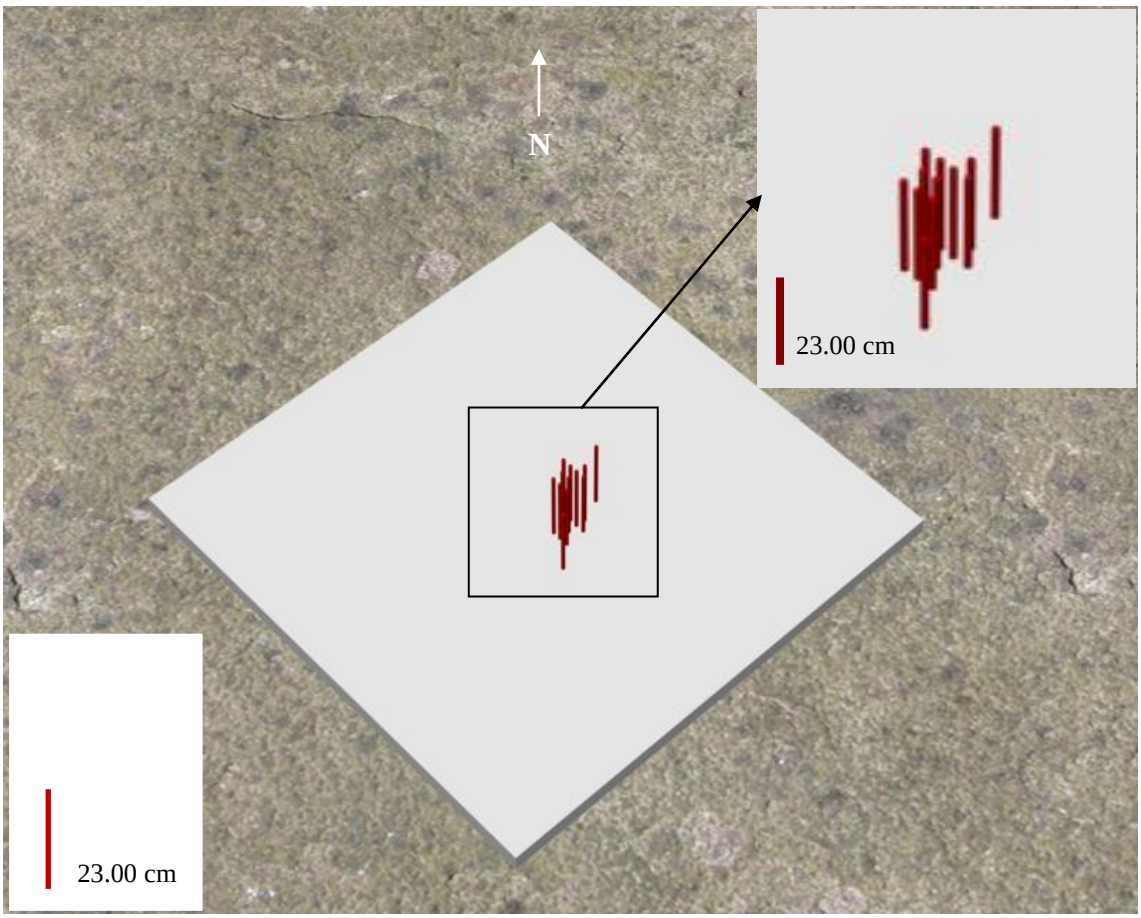

Fig. 4.3 Time-mediated growth of ramets in *Scirpus grossus* grown in unfertilized peat soil (F0) 1 month after planting of the mother plant. ▏, emerged ramets in the 1st month developed using AutoCAD 10. ↑N denotes geographical north.

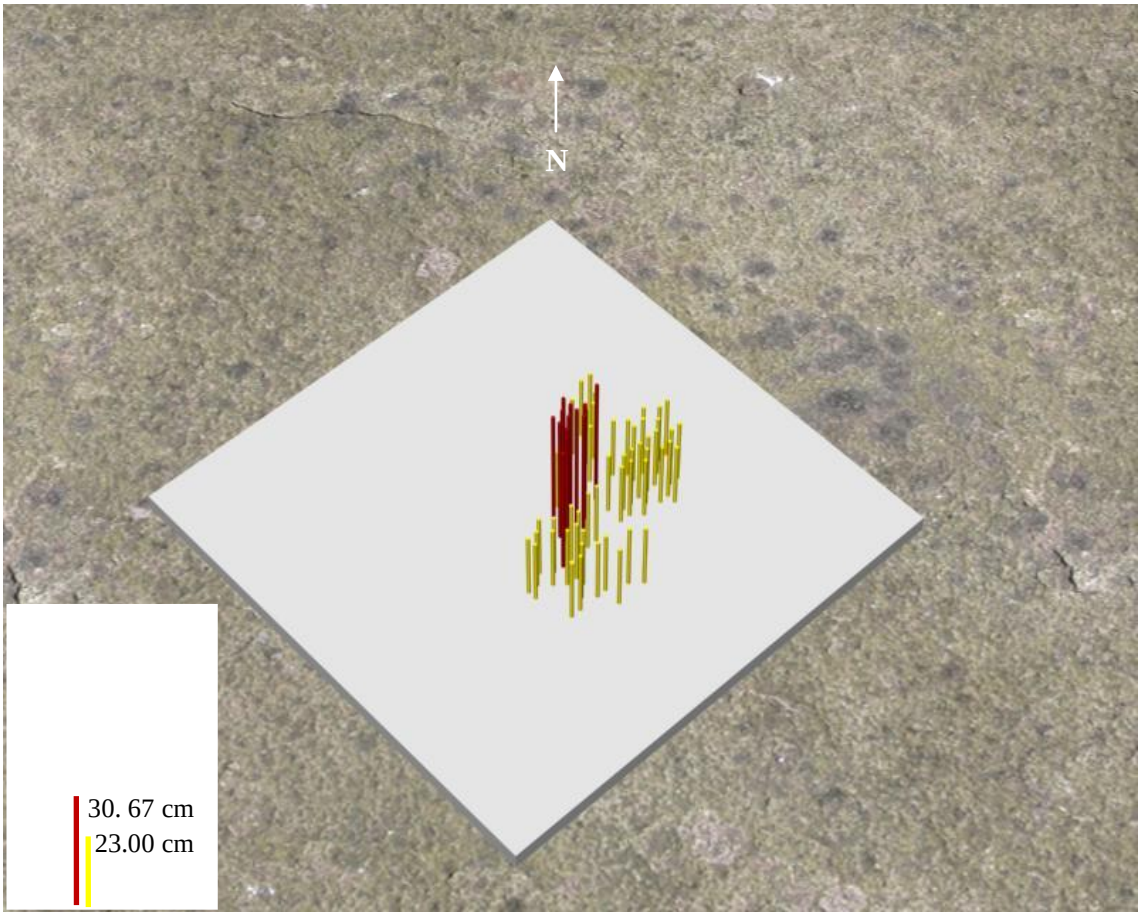

Fig. 4.4 Time-mediated growth of ramets in *Scirpus grossus* grown in unfertilized peat soil (F0) 2 months after planting of the mother plant. ▏, emerged ramets in the 1st month; ▏, emerged ramets in the 2nd month developed using AutoCAD 10. ↑N denotes geographical north.

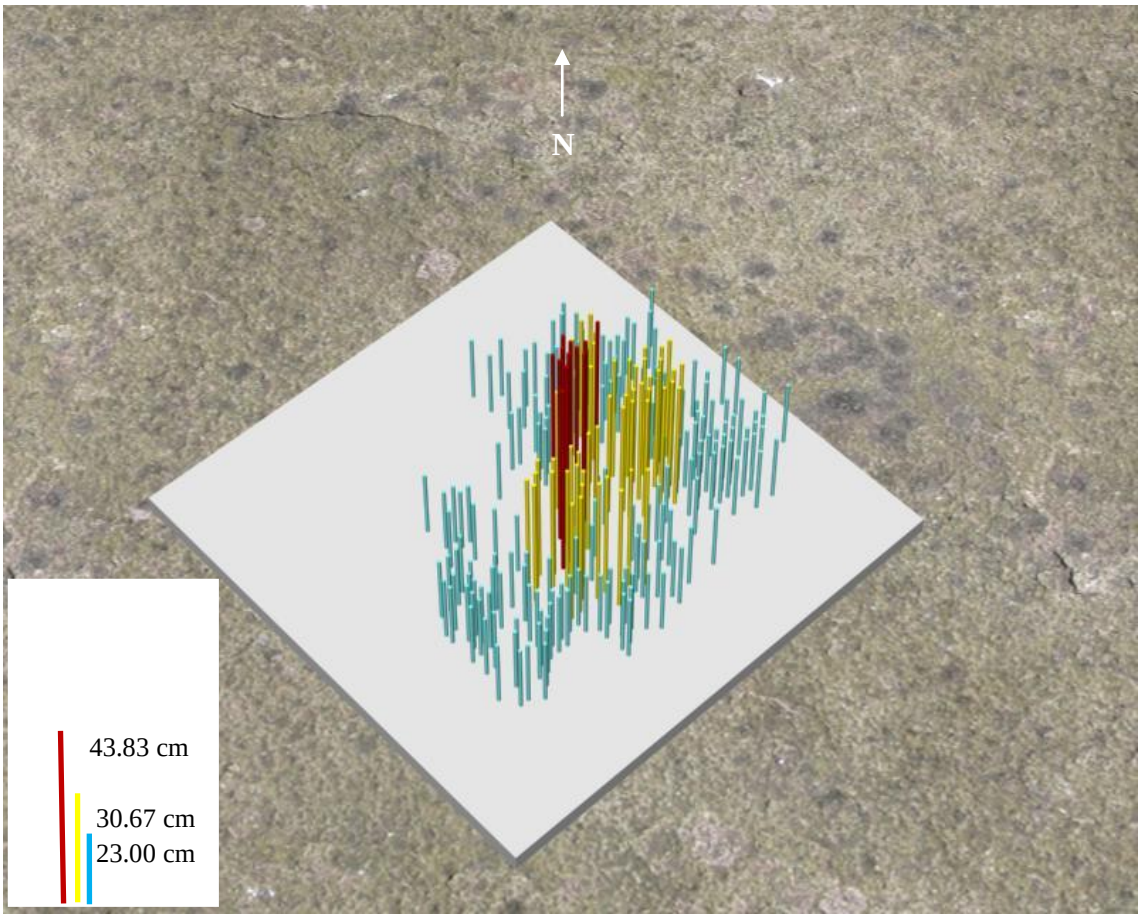

Fig. 4.5 Time-mediated growth of ramets in *Scirpus grossus* grown in unfertilized peat soil (F0) 3 months after planting of the mother plant. |, emerged ramets in the 1st month; |, emerged ramets in the 2nd month; |, emerged ramets in the 3rd month developed using AutoCAD 10. ↑N denotes geographical north.

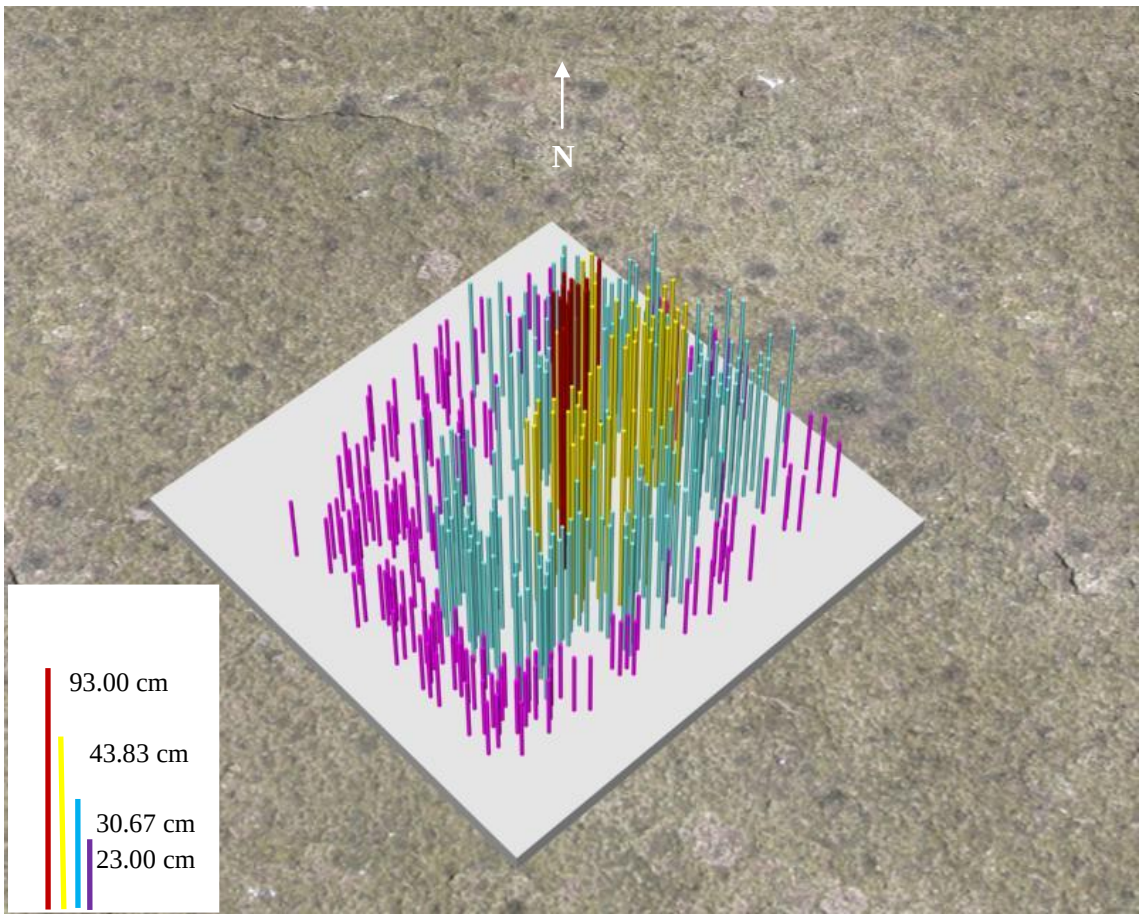

Fig. 4.6 Time-mediated growth of ramets in *Scirpus grossus* grown in unfertilized peat soil (F0) 4 months after planting of the mother plant. ▏, emerged ramets in the 1st month; ▏, emerged ramets in the 2nd month; ▏, emerged ramets in the 3rd month; ▏, emerged ramets in the 4th month developed using AutoCAD 10. ↑N denotes geographical north.

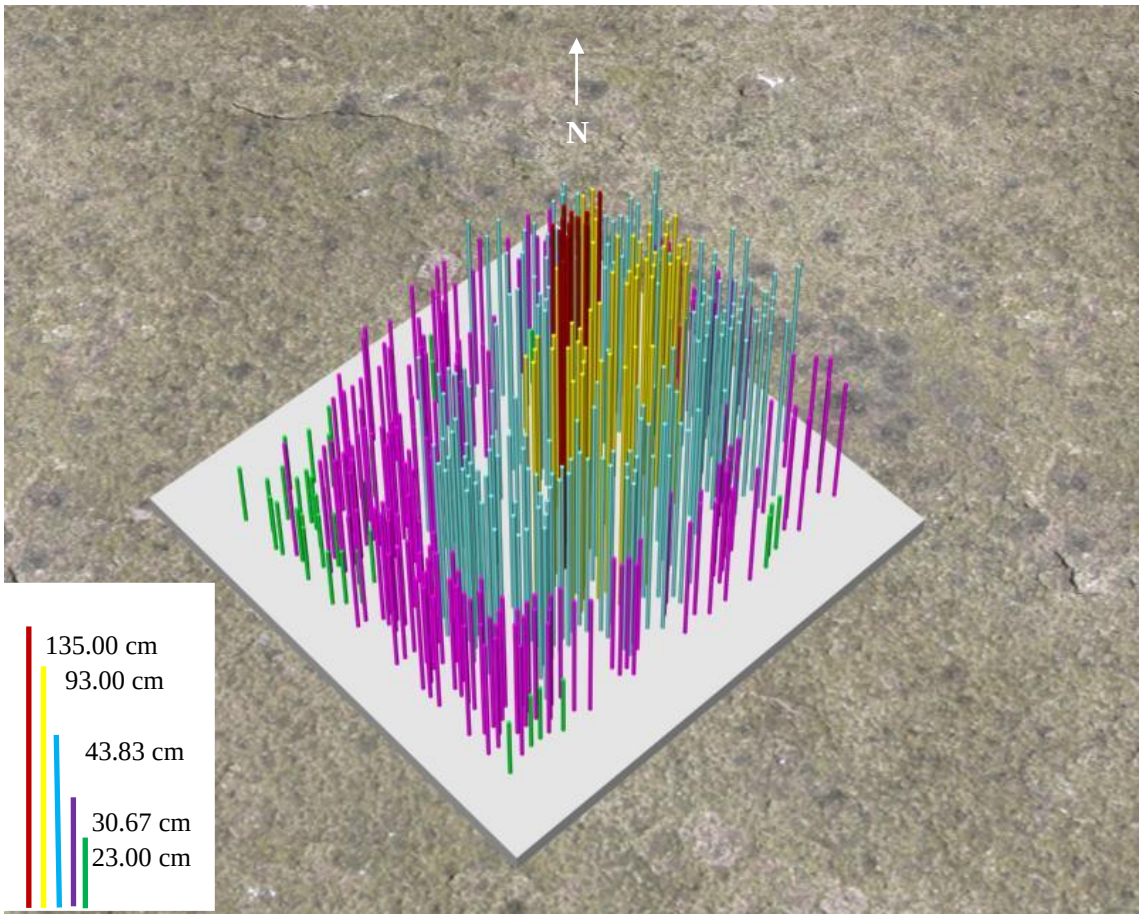

Fig. 4.7 Time-mediated growth of ramets in *Scirpus grossus* grown in unfertilized peat soil (F0) 5 months after planting of the mother plant. |, emerged ramets in the 1st month; |, emerged ramets in the 2nd month; |, emerged ramets in the 3rd month; |, emerged ramets in the 4th month; |, emerged ramets in the 5th month developed using AutoCAD 10.↑N denotes geographical north.

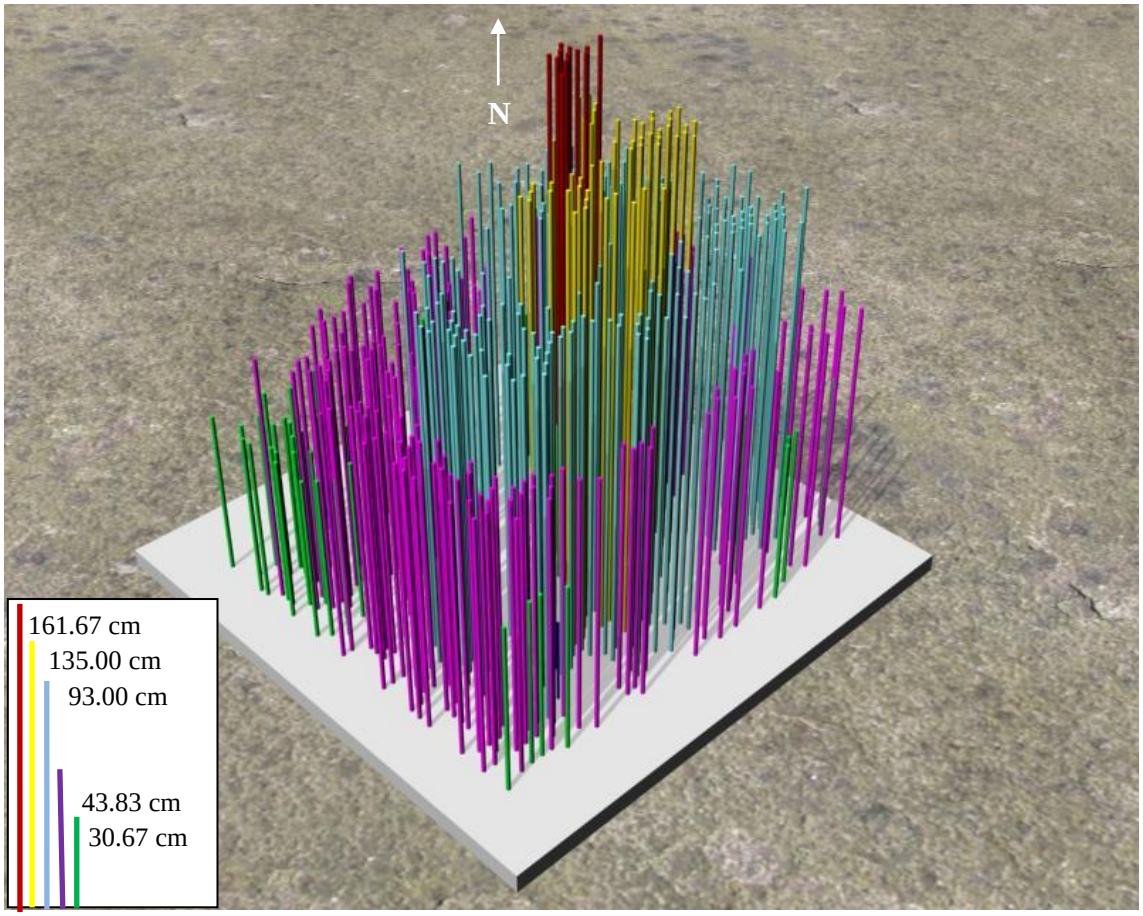

Fig. 4.8 Time-mediated growth of ramets in *Scirpus grossus* grown in unfertilized peat soil (F0) 6 months after planting of the mother plant. |, emerged ramets in the 1st month; |, emerged ramets in the 2nd month; |, emerged ramets in the 3rd month; |, emerged ramets in the 4th month; |, emerged ramets in the 5th month; and |, emerged ramets in the 6th month developed using AutoCAD 10. ↑N denotes geographical north.

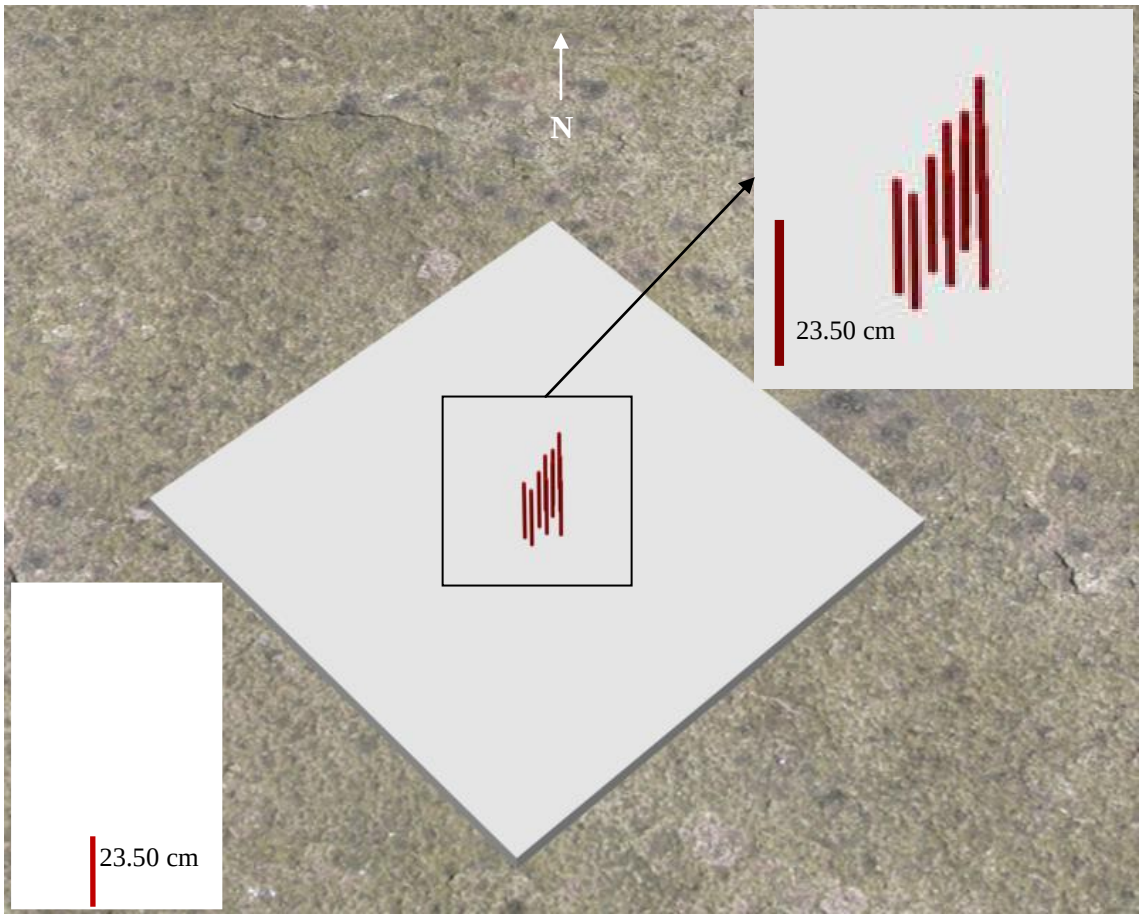

Fig. 4.9 Time-mediated growth of ramets in *Scirpus grossus* grown in fertilized peat soil (F1) 1 month after planting of the mother plant. ⎪, emerged ramets in the 1st month developed using AutoCAD 10. ↑N denotes geographical north.

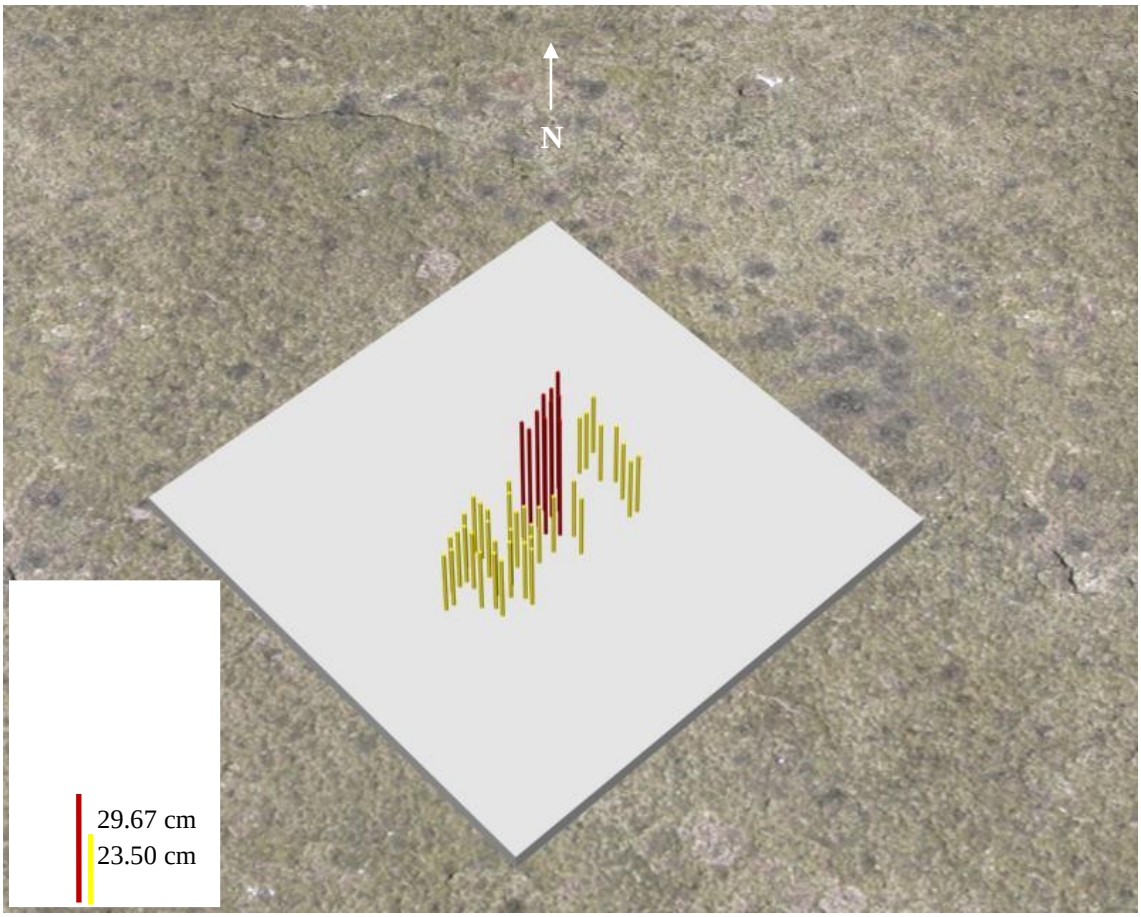

Fig. 4.10 Time-mediated growth of ramets in *Scirpus grossus* grown in fertilized peat soil (F1) 2 months after planting of the mother plant. ▏, emerged ramets in the 1st month; ▏, emerged ramets in the 2nd month developed using AutoCAD 10. ↑N denotes geographical north.

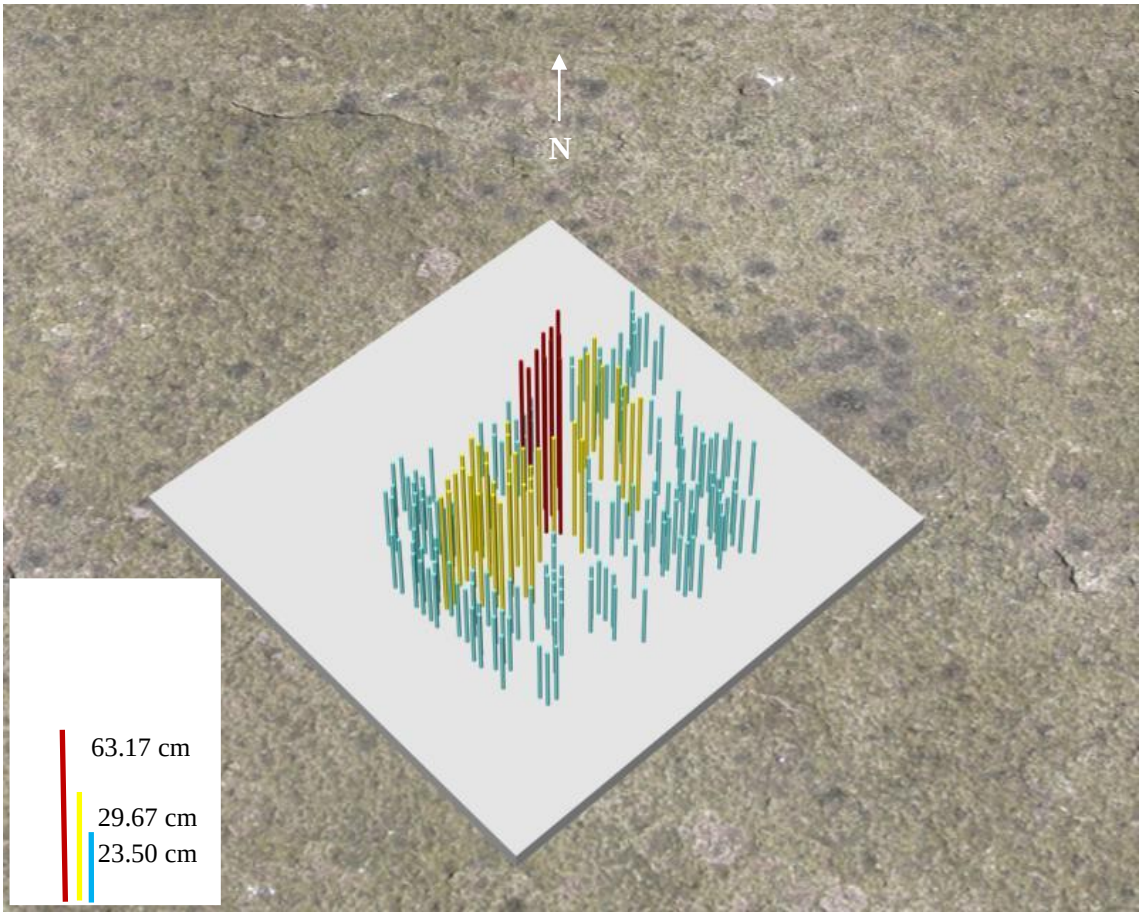

Fig. 4.11 Time-mediated growth of ramets in *Scirpus grossus* grown in fertilized peat soil (F1) 3 months after planting of the mother plant. |, emerged ramets in the 1st month; |, emerged ramets in the 2nd month; |, emerged ramets in the 3rd month developed using AutoCAD 10. ↑N denotes geographical north.

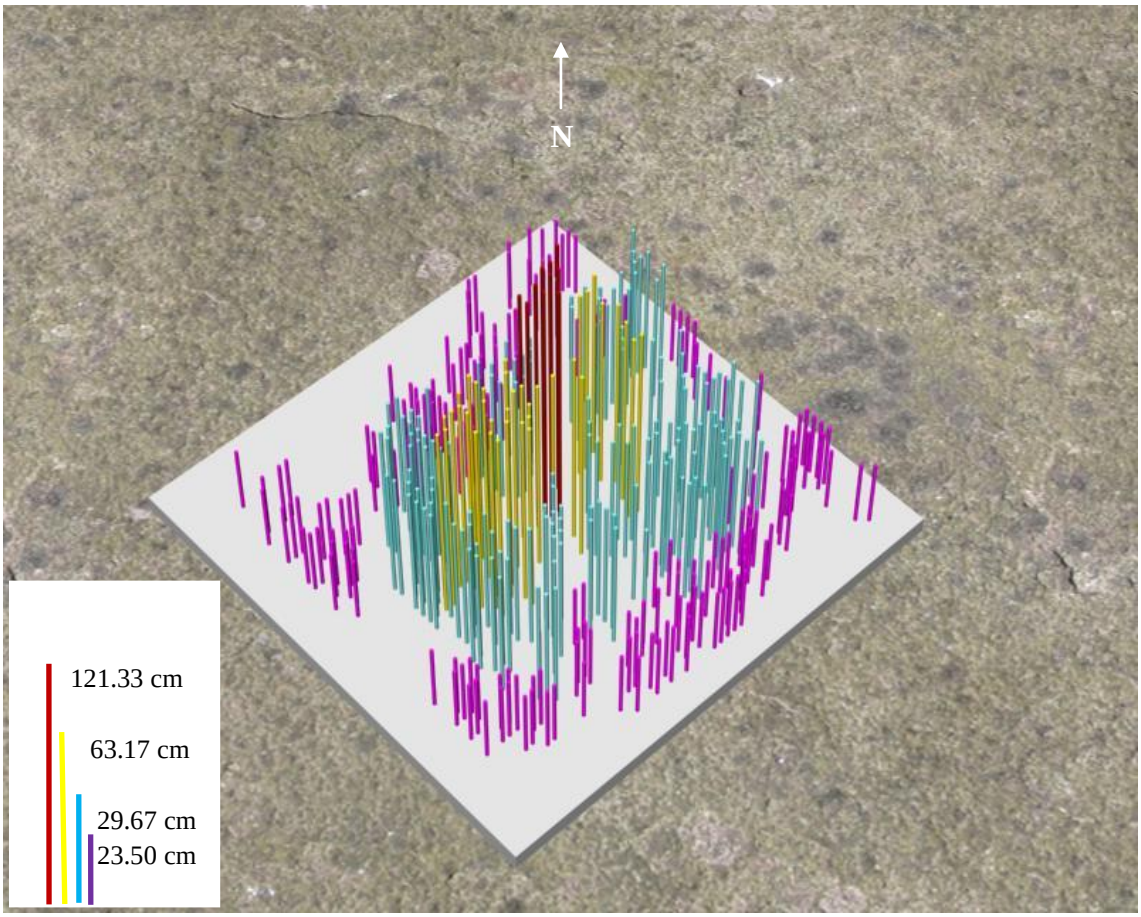

Fig. 4.12 Time-mediated growth of ramets in *Scirpus grossus* grown in fertilized peat soil (F1) 4 months after planting of the mother plant. ▏, emerged ramets in the 1st month; ▏, emerged ramets in the 2nd month; ▏, emerged ramets in the 3rd month; ▏, emerged ramets in the 4th month developed using AutoCAD 10. ↑N denotes geographical north.

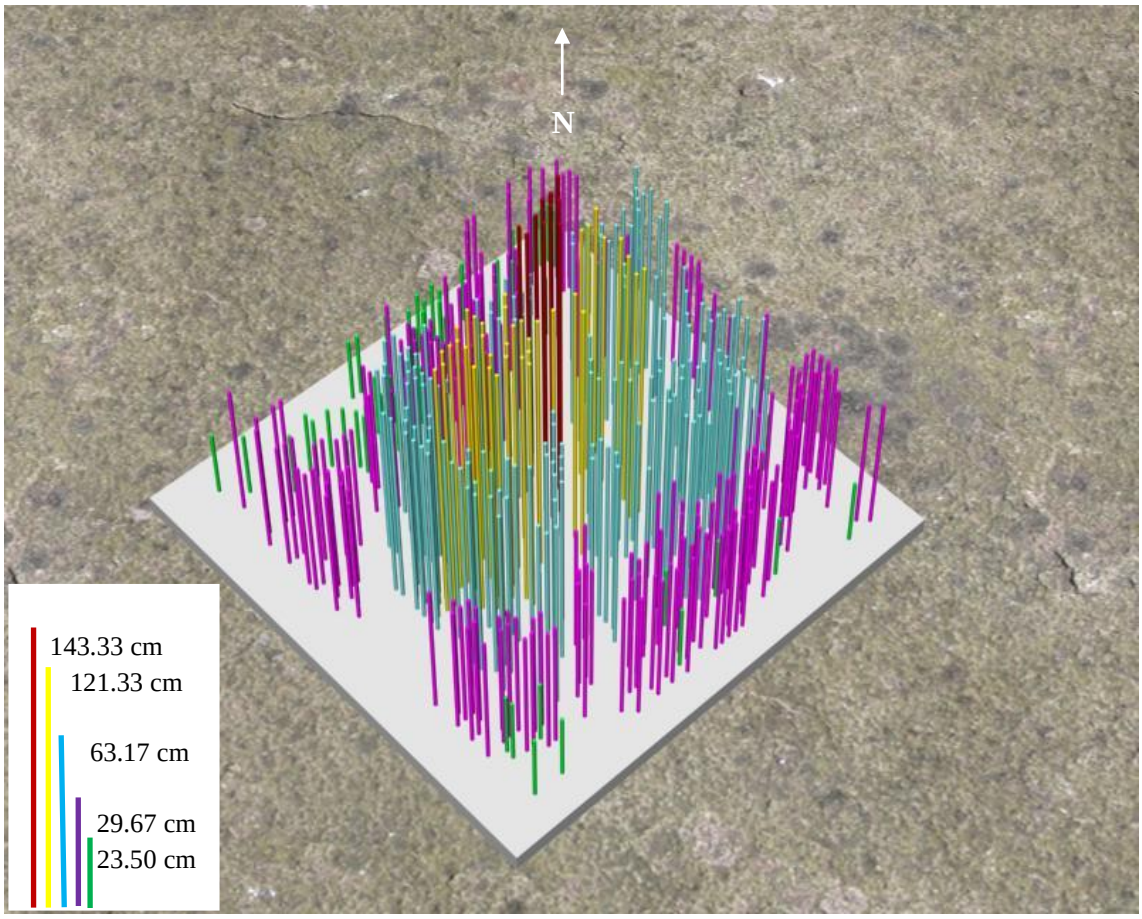

Fig. 4.13 Time-mediated growth of ramets in *Scirpus grossus* grown in fertilized peat soil (F1) 5 months after planting of the mother plant. |, emerged ramets in the 1st month; |, emerged ramets in the 2nd month; |, emerged ramets in the 3rd month; |, emerged ramets in the 4th month; |, emerged ramets in the 5th month developed using AutoCAD 10. ↑N denotes geographical north.

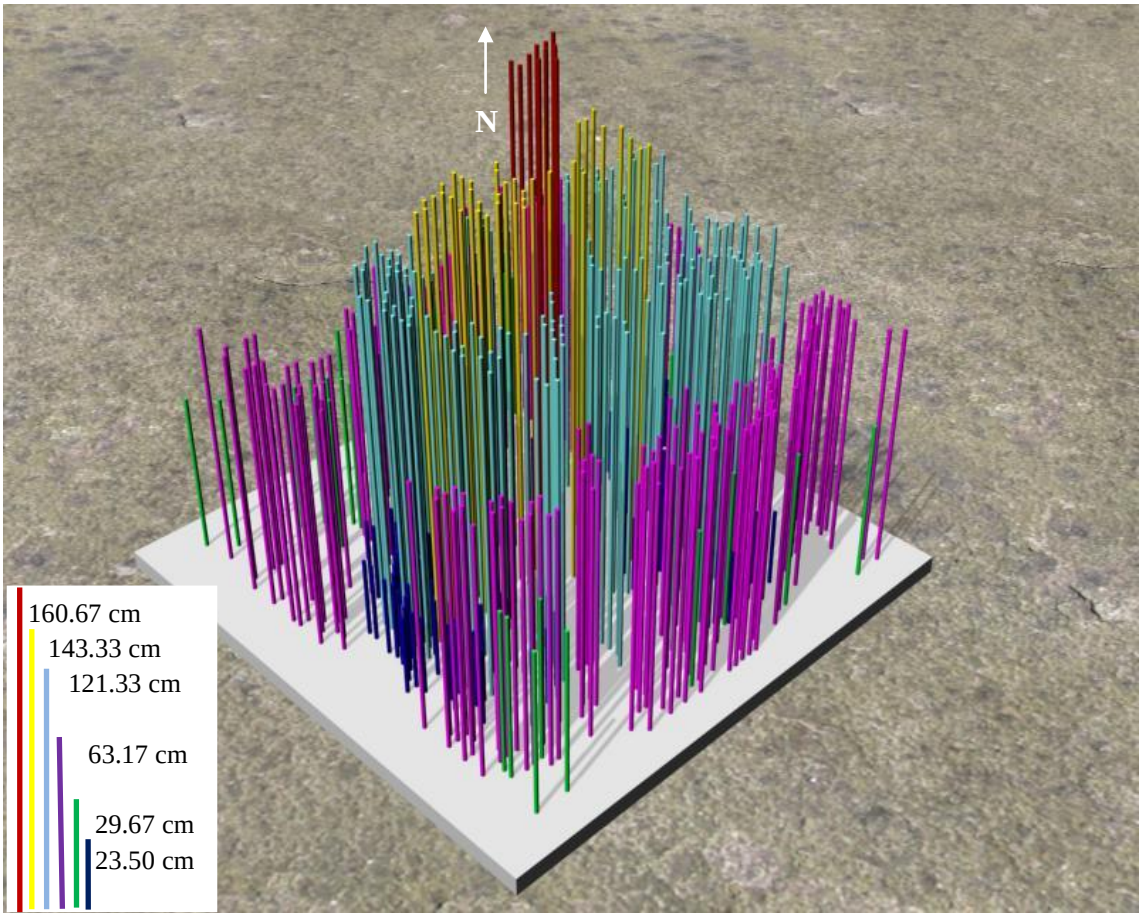

Fig. 4.14 Time-mediated growth of ramets in *Scirpus grossus* grown in fertilized peat soil (F1) 6 months after planting of the mother plant. |, emerged ramets in the 1st month; |, emerged ramets in the 2nd month; |, emerged ramets in the 3rd month; |, emerged ramets in the 4th month; |, emerged ramets in the 5th month; and |, emerged ramets in the 6th month developed using AutoCAD 10. ↑N denotes geographical north.

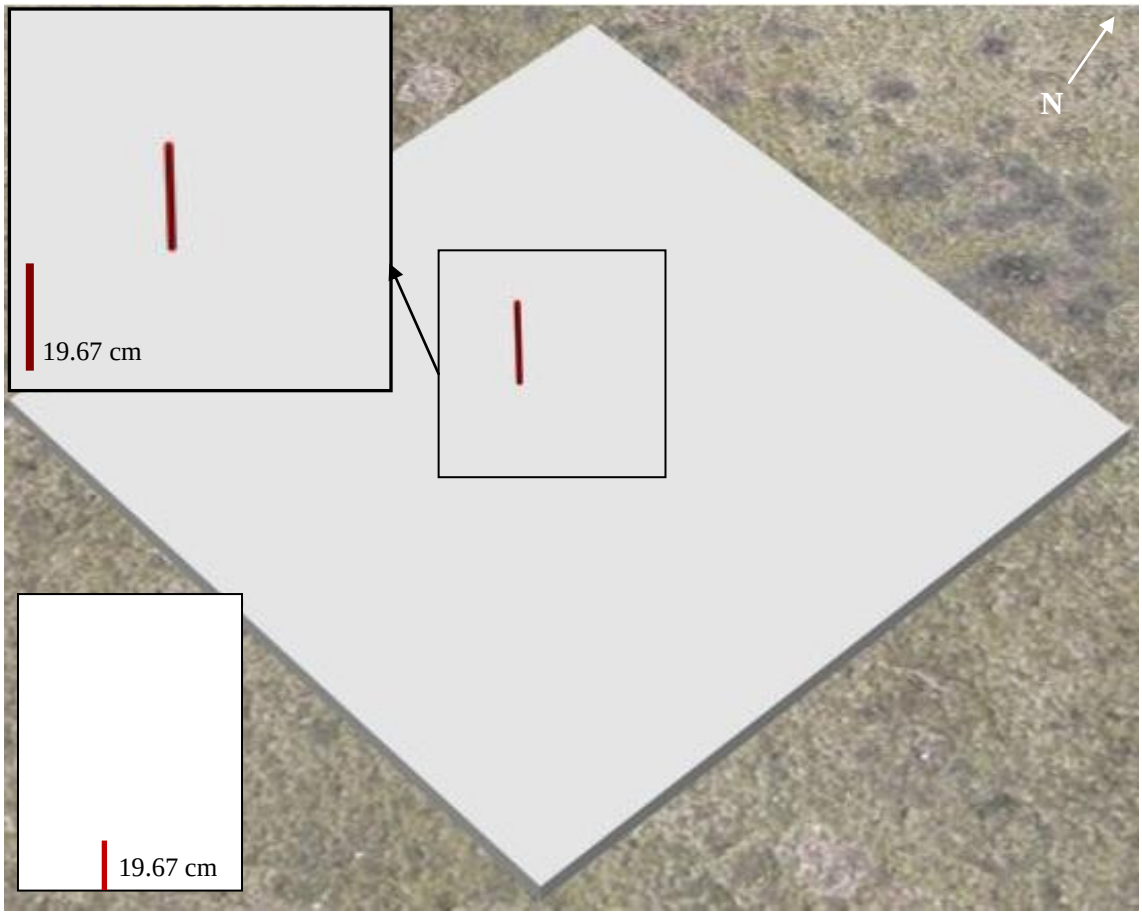

Fig. 4.15 Time-mediated growth of ramets in *Scirpus grossus* grown in unfertilized paddy soil (F0) 1 month after planting of the mother plant. ⏐, emerged ramets in the 1st month developed using AutoCAD 10. ↑N denotes geographical north.

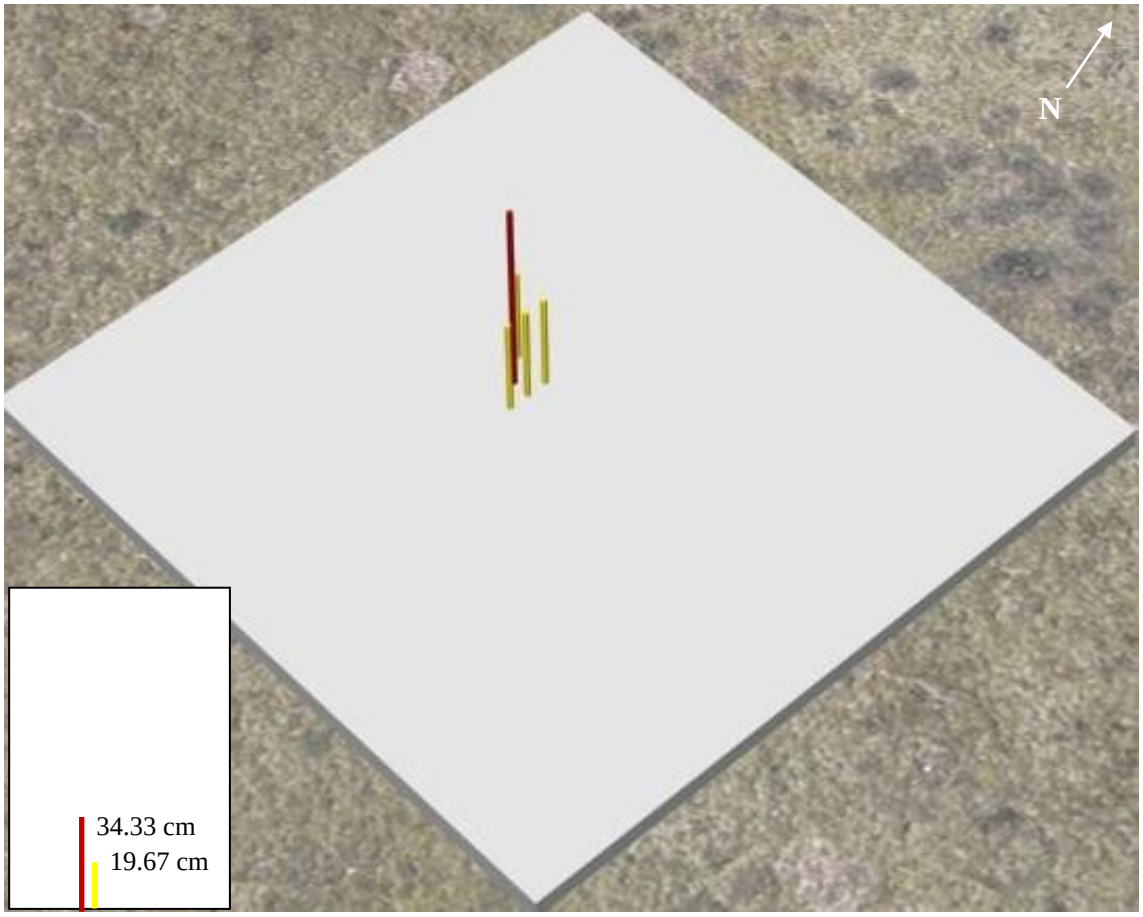

Fig. 4.16 Time-mediated growth of ramets in *Scirpus grossus* grown in unfertilized paddy soil (F0) 2 months after planting of the mother plant. ▏, emerged ramets in the 1st month; ▏, emerged ramets in the 2nd month developed using AutoCAD 10. ↑N denotes geographical north.

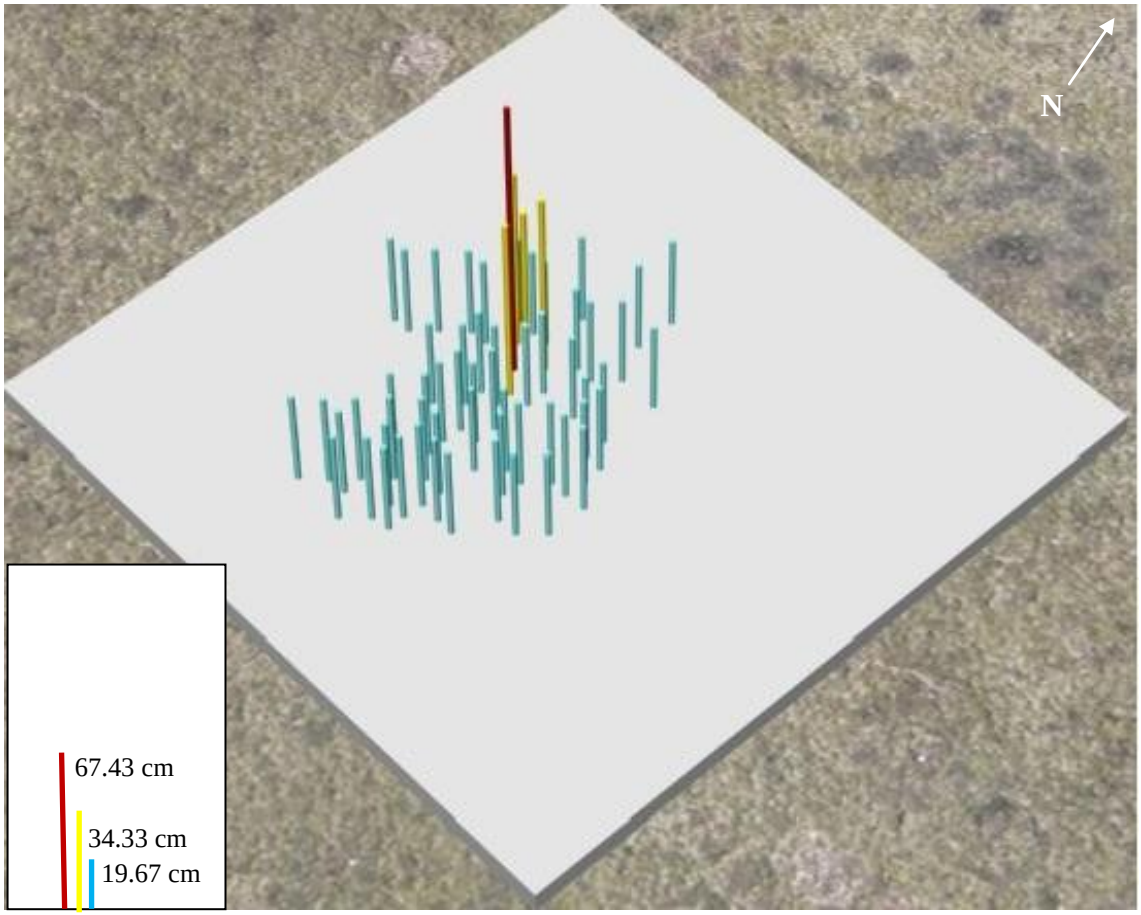

Fig. 4.17 Time-mediated growth of ramets in *Scirpus grossus* grown in unfertilized paddy soil (F0) 3 months after planting of the mother plant. |, emerged ramets in the 1st month; |, emerged ramets in the 2nd month; |, emerged ramets in the 3rd month developed using AutoCAD 10. ↑N denotes geographical north.

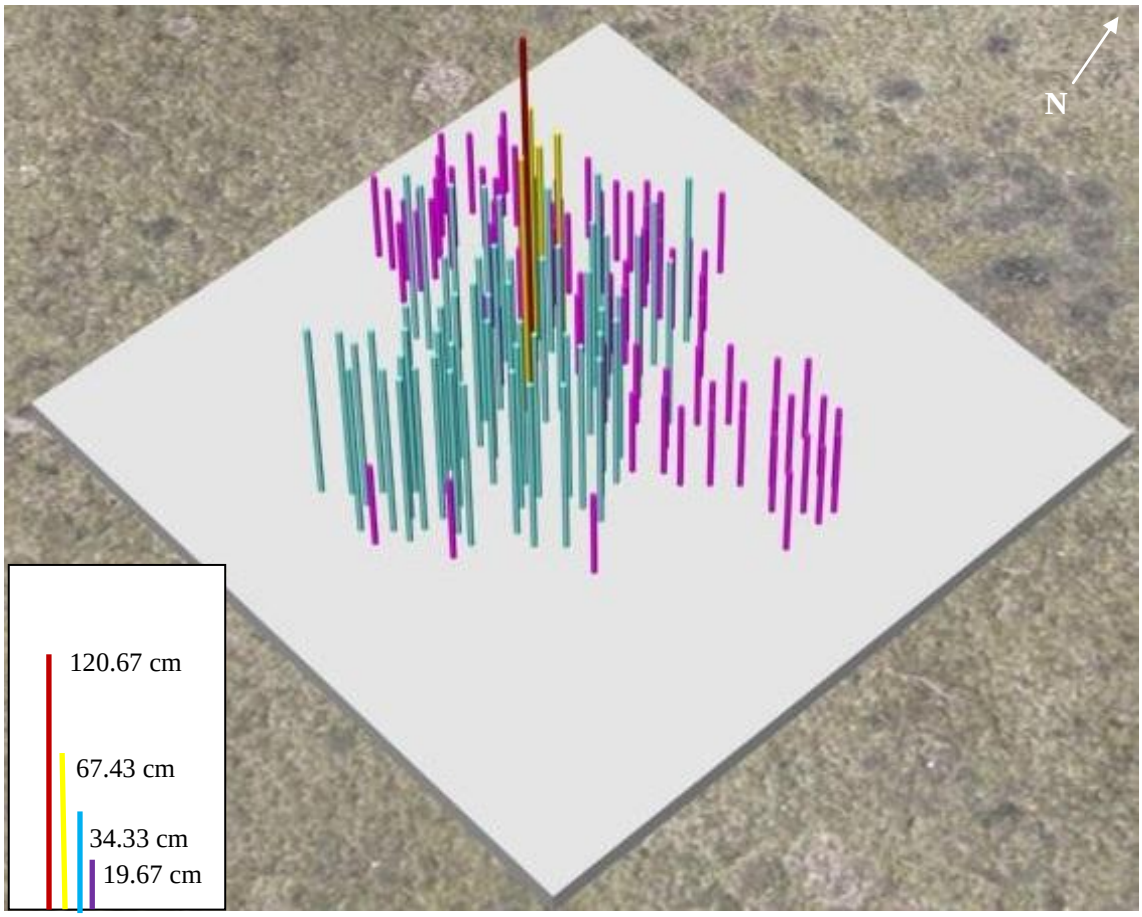

Fig. 4.18 Time-mediated growth of ramets in *Scirpus grossus* grown in unfertilized paddy soil (F0) 4 months after planting of the mother plant. |, emerged ramets in the 1st month; |, emerged ramets in the 2nd month; |, emerged ramets in the 3rd month; |, emerged ramets in the 4th month developed using AutoCAD 10. ↑N denotes geographical north.

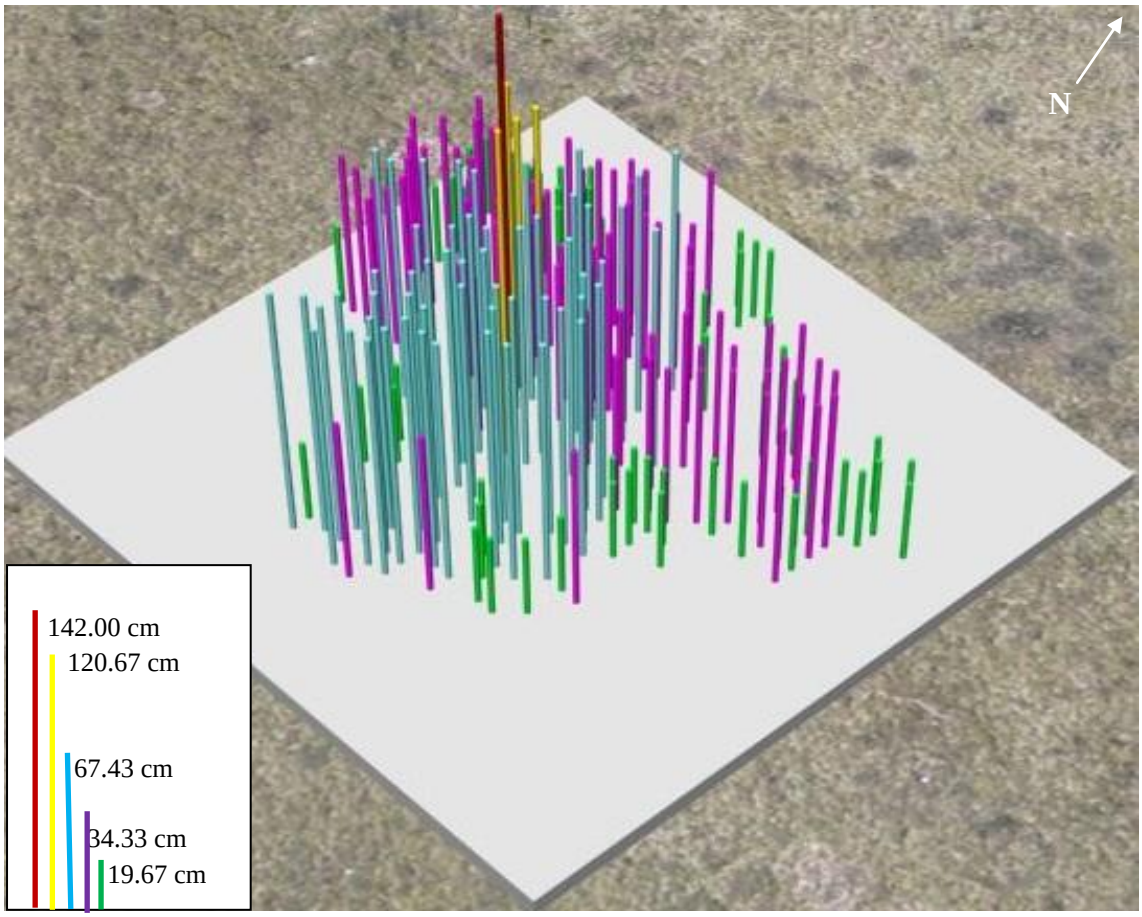

Fig. 4.19 Time-mediated growth of ramets in *Scirpus grossus* grown in unfertilized paddy soil (F0) 5 months after planting of the mother plant. |, emerged ramets in the 1st month; |, emerged ramets in the 2nd month; |, emerged ramets in the 3rd month; |, emerged ramets in the 4th month; |, emerged ramets in the 5th month developed using AutoCAD 10. ↑N denotes geographical north.

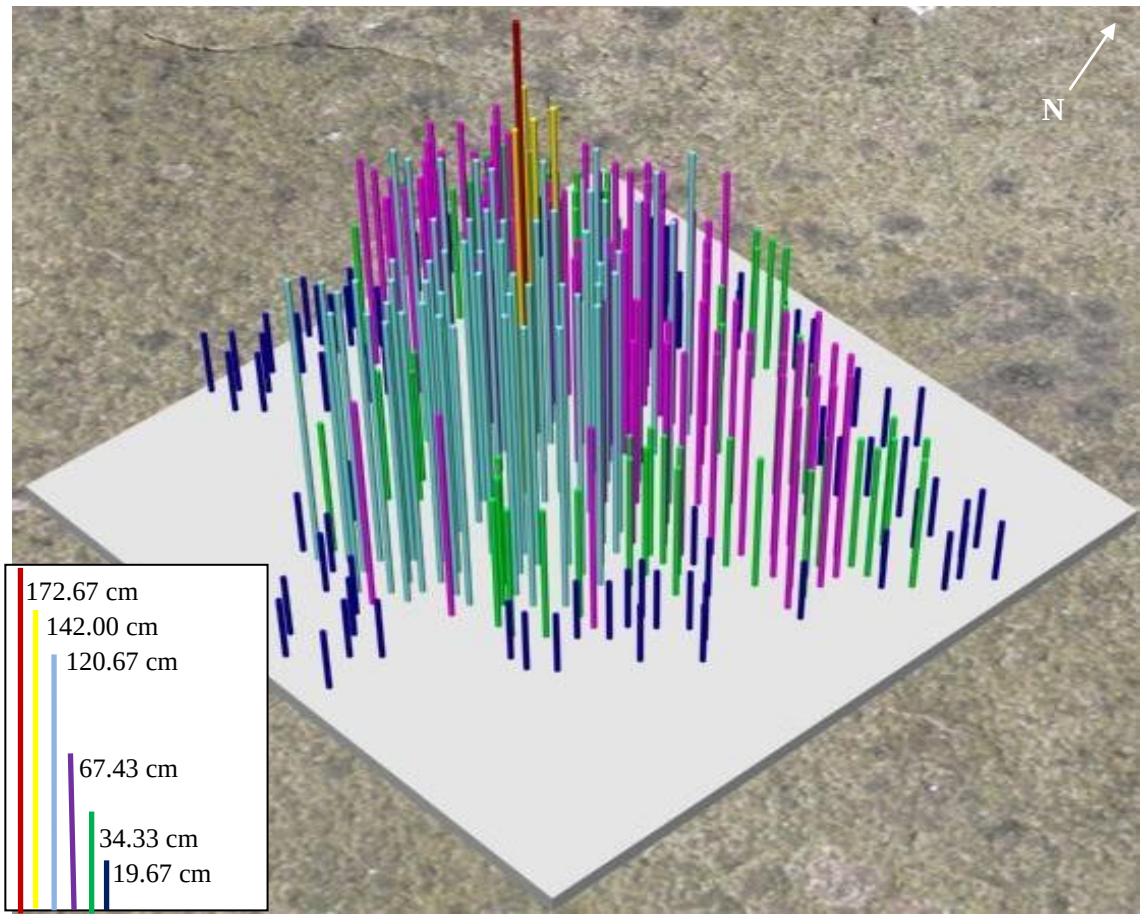

Fig. 4.20 Time-mediated growth of ramets in *Scirpus grossus* grown in unfertilized paddy soil (F0) 6 months after planting of the mother plant. |, emerged ramets in the 1st month; |, emerged ramets in the 2nd month; |, emerged ramets in the 3rd month; |, emerged ramets in the 4th month; |, emerged ramets in the 5th month; and |, emerged ramets in the 6th month developed using AutoCAD 10. ↑N denotes geographical north.

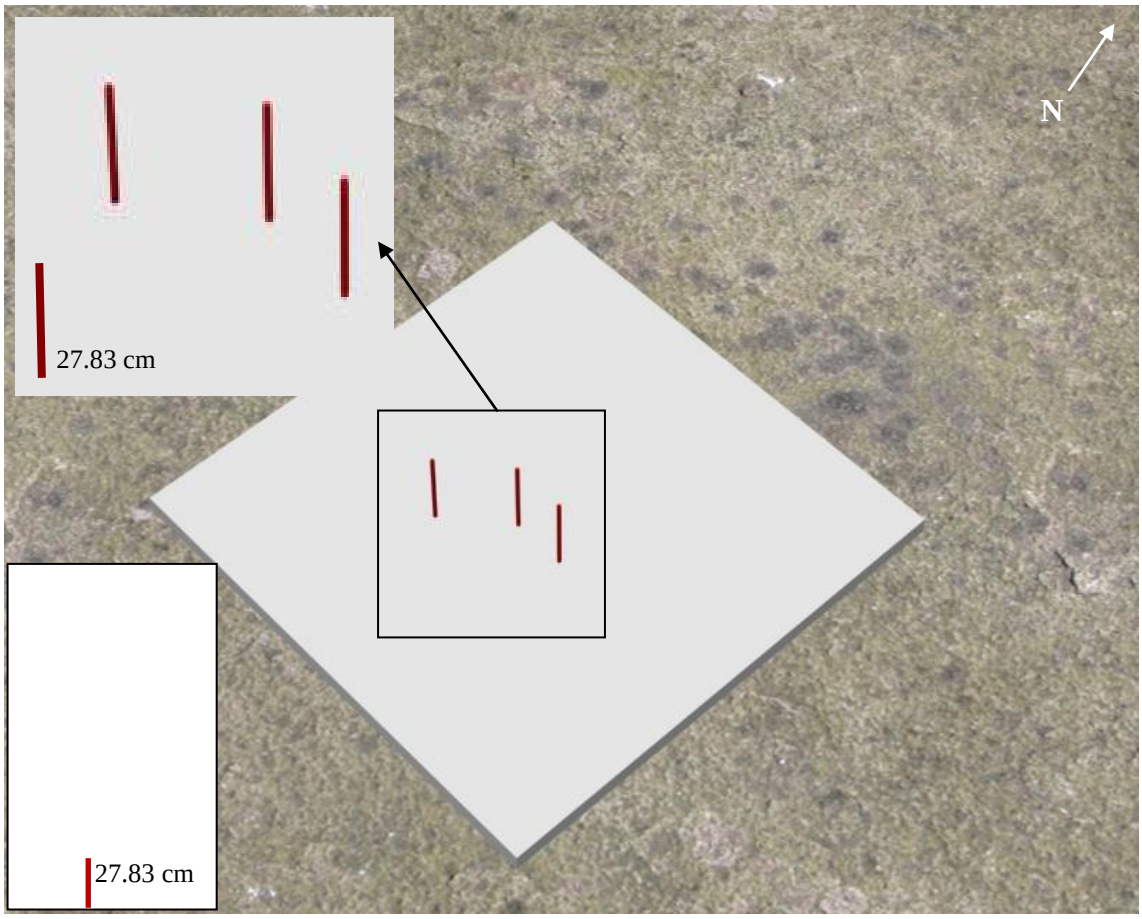

Fig. 4.21 Time-mediated growth of ramets in *Scirpus grossus* grown in fertilized paddy soil (F1) 1 month after planting of the mother plant. |, emerged ramets in the 1st month developed using AutoCAD 10. ↑N denotes geographical north.

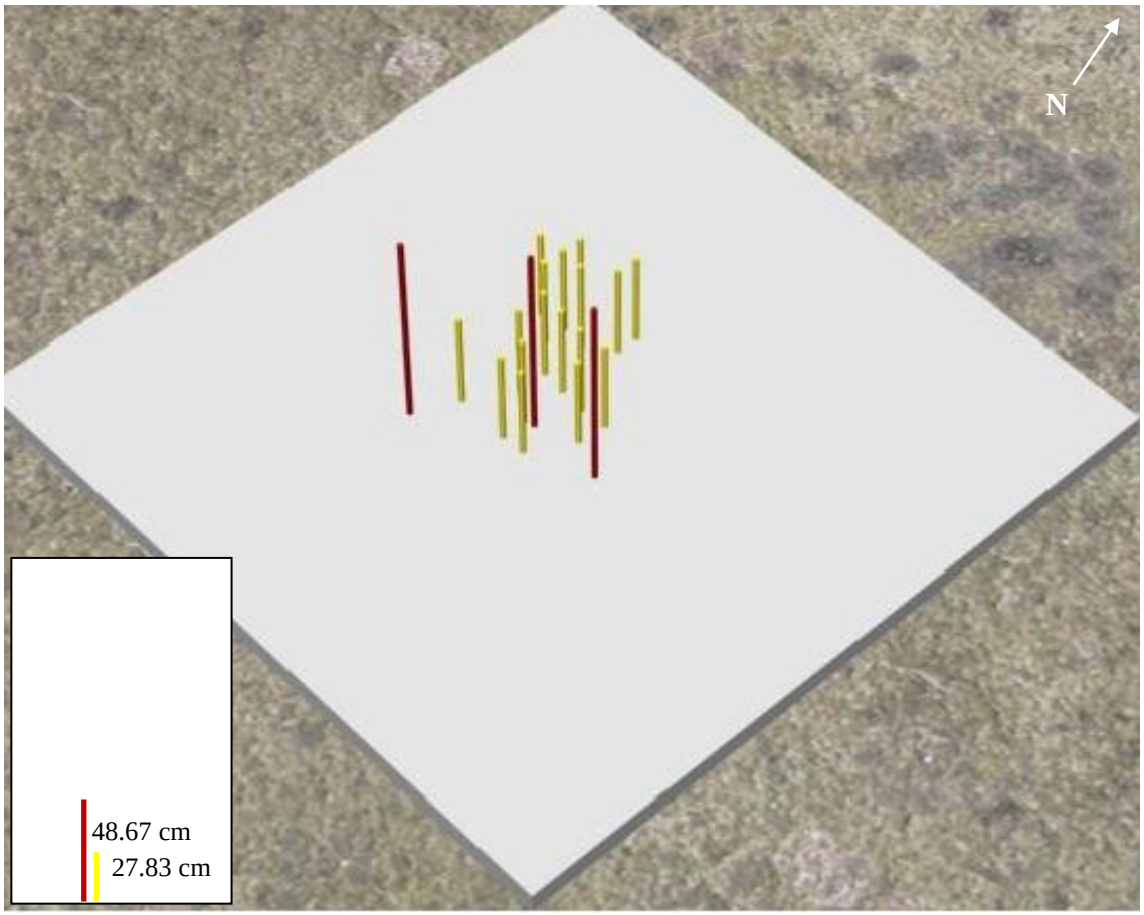

Fig. 4.22 Time-mediated growth of ramets in *Scirpus grossus* grown in fertilized paddy soil (F1) 2 months after planting of the mother plant. ▏, emerged ramets in the 1st month; ▏, emerged ramets in the 2nd month developed using AutoCAD 10. ↑N denotes geographical north.

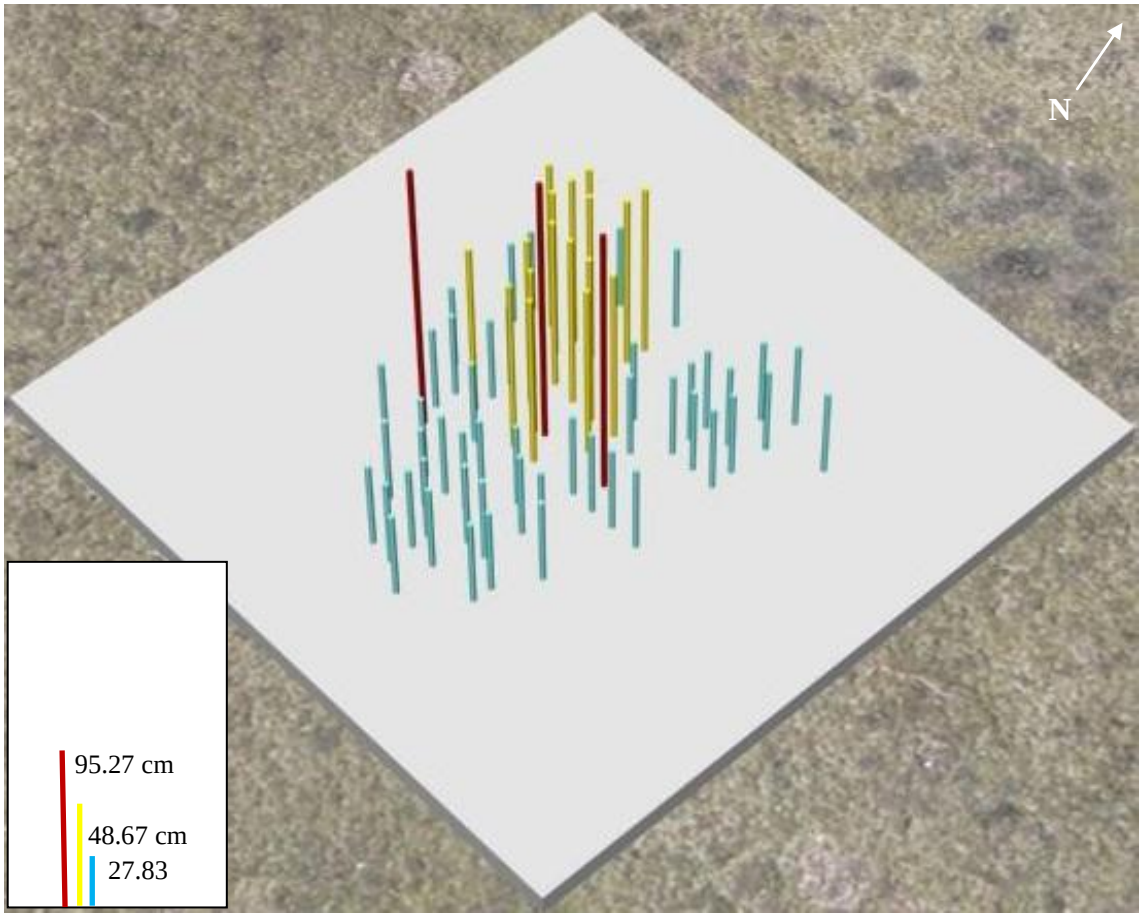

Fig. 4.23 Time-mediated growth of ramets in *Scirpus grossus* grown in fertilized paddy soil (F1) 3 months after planting of the mother plant. |, emerged ramets in the 1st month; |, emerged ramets in the 2nd month; |, emerged ramets in the 3rd month developed using AutoCAD 10. ↑N denotes geographical north.

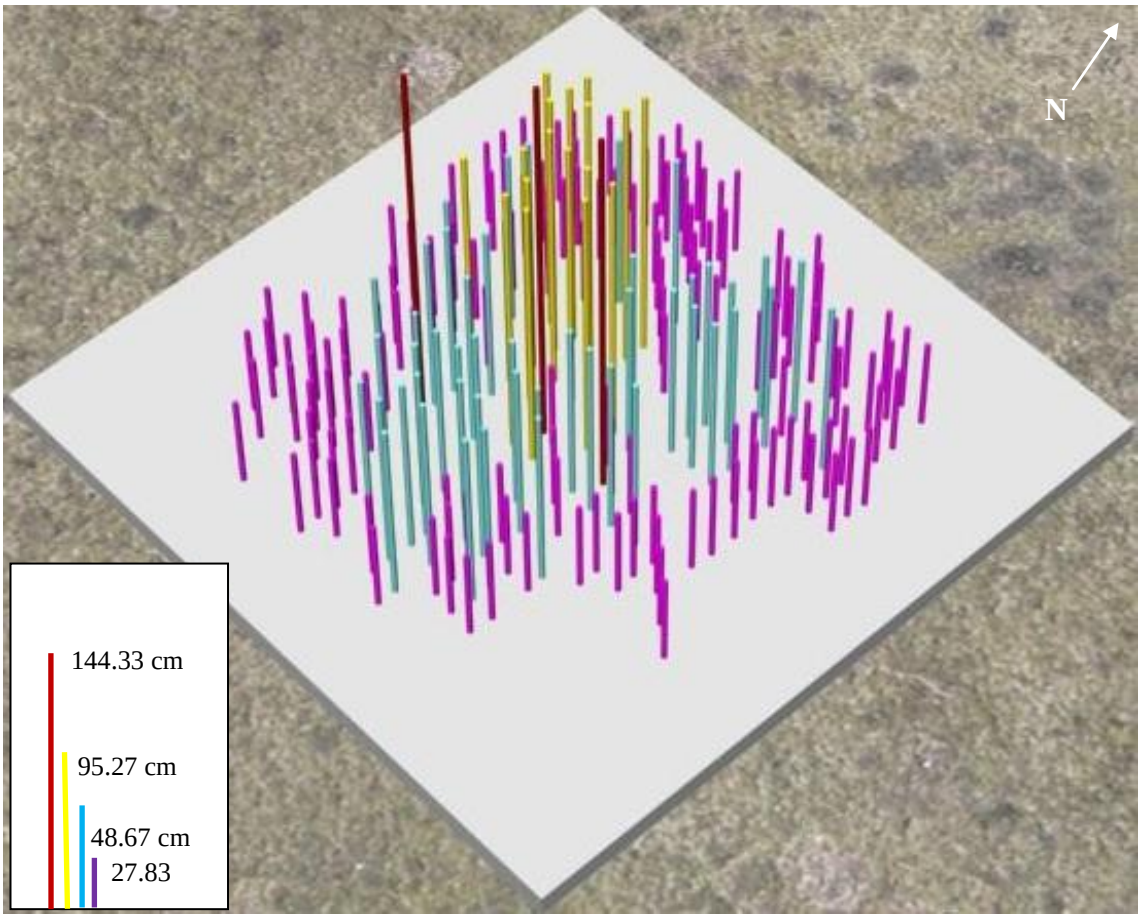

Fig. 4.24 Time-mediated growth of ramets in *Scirpus grossus* grown in fertilized paddy soil (F1) 4 months after planting of the mother plant. ▏, emerged ramets in the 1st month; ▏, emerged ramets in the 2nd month; ▏, emerged ramets in the 3rd month; ▏, emerged ramets in the 4th month developed using AutoCAD 10. ↑N denotes geographical north.

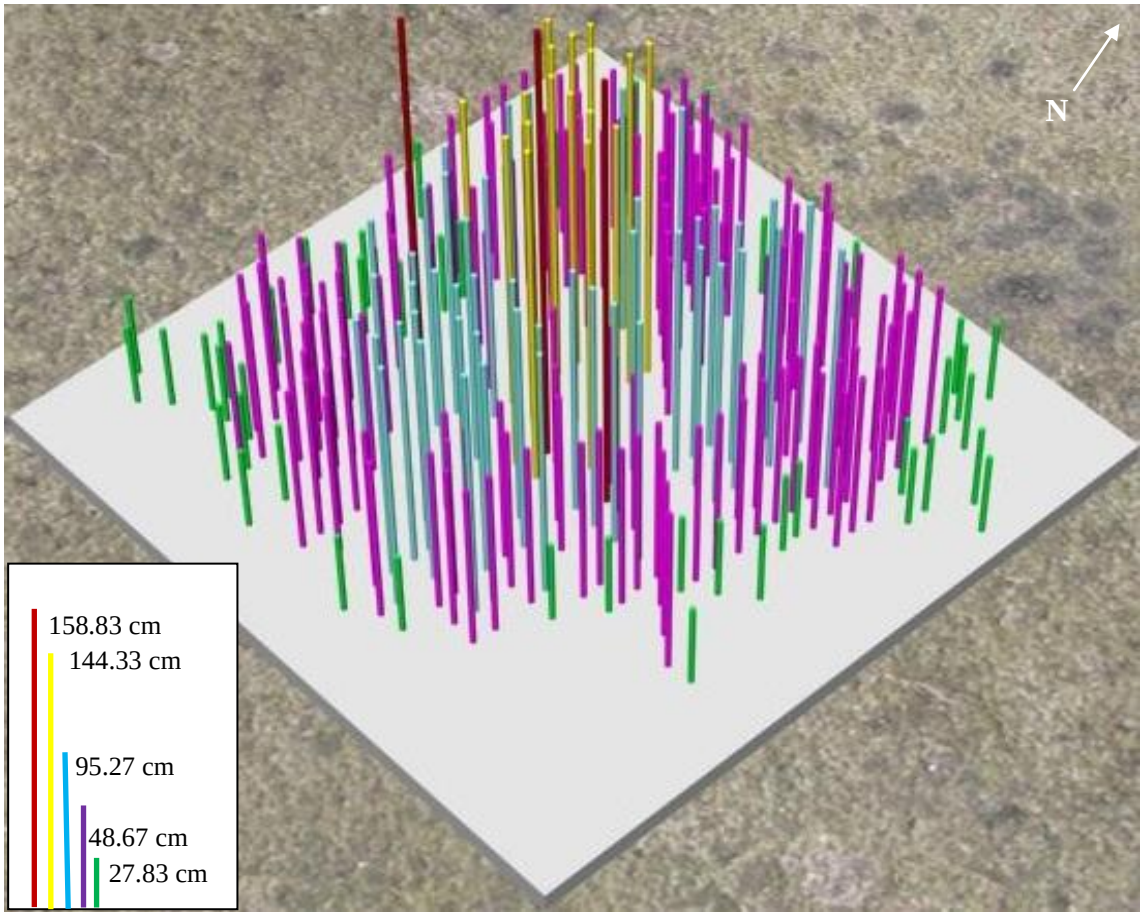

Fig. 4.25 Time-mediated growth of ramets in *Scirpus grossus* grown in fertilized paddy soil (F1) 5 months after planting of the mother plant. |, emerged ramets in the 1st month; |, emerged ramets in the 2nd month; |, emerged ramets in the 3rd month; |, emerged ramets in the 4th month; |, emerged ramets in the 5th month developed using AutoCAD 10. ↑N denotes geographical north.

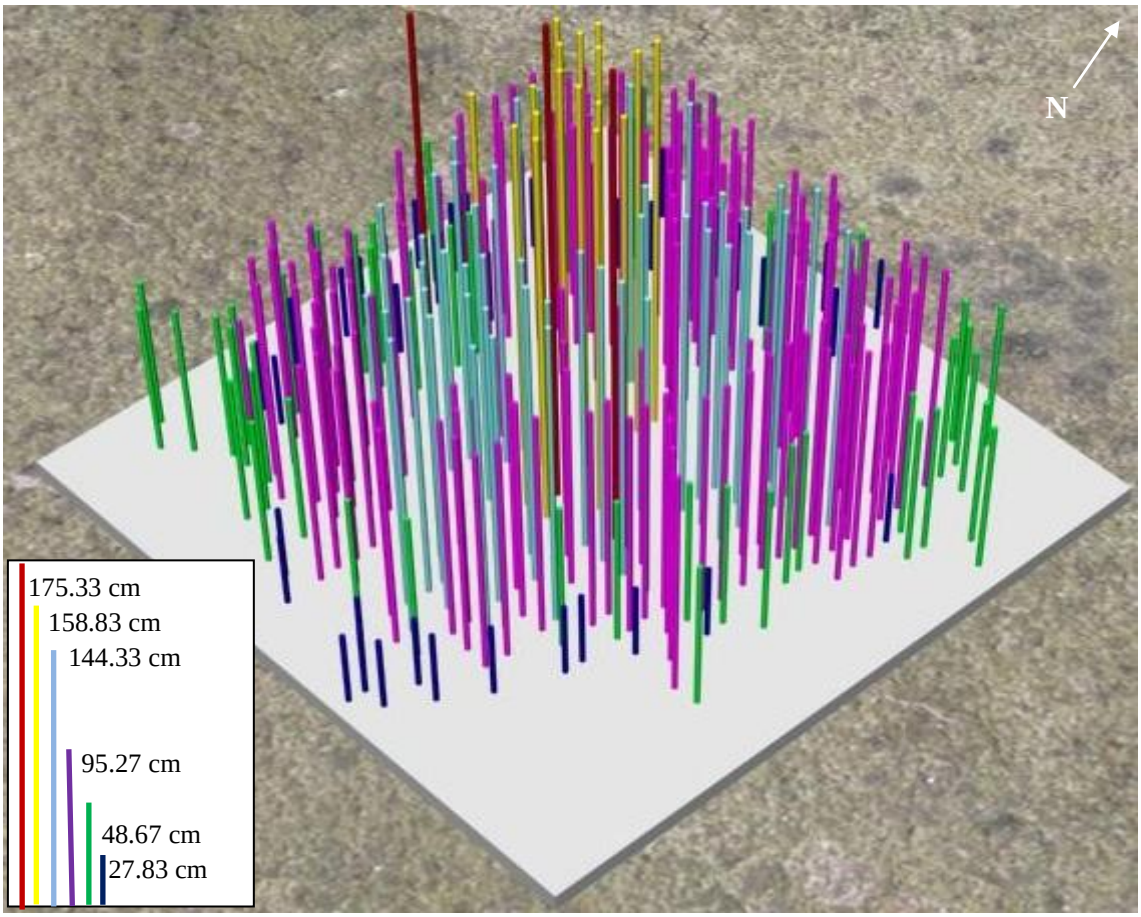

Fig. 4.26 Time-mediated growth of ramets in *Scirpus grossus* grown in fertilized paddy soil (F1) 6 months after planting of the mother plant. |, emerged ramets in the 1st month; |, emerged ramets in the 2nd month; |, emerged ramets in the 3rd month; |, emerged ramets in the 4th month; |, emerged ramets in the 5th month; and |, emerged ramets in the 6th month developed using AutoCAD 10. ↑N denotes geographical north.

4.3.3 Dispersion analyses of *Scirpus grossus* ramets

4.3.3.1 Dispersion analyses of *Scirpus grossus* ramets in both fertilized and unfertilized peat and paddy soils

Table 4.3 shows the circular statistics r (concentration), s (angular deviation), Rayleigh's R and Rayleigh's z computed on the emerged ramets of *S. grossus*.

Results of Rayleigh's z test showed momentous niggardly direction of ramets emergence for all replicates in the fertilized plots ($p > 0.01$). Significant mean direction is obtained only for replicate R1 for the unfertilised plots. No significant mean direction for replicates R2 and R3 of the unfertilised plots means that ramets emergence is distributed uniformly around the circle, that is originating from the mother plant. They occur when s, the dispersion given by the angular deviation is near the maximum (where $0 < s < 83.01$). Dispersion analysis of ramets by circular statistics on *S. grossus* generated no special preferences in the direction of modules or emerged ramets as explained by the Rayleigh's r, Rayleigh's z, and mean angle of dispersion (Table 4.3). However, there were heavier concentrations of ramets in the eastern sector of the plot, presumably due to phototropic effect of sunlight (Fig. 4.27).

In table 4.4 showed the circular statistics *r* (concentration), *s* (angular deviation), Rayleigh's *R* and Rayleigh's *z* computed on the emerged ramets of *S. grossus.*

Results of Rayleigh's z test showed significant mean direction of ramets emergence for all replicates in the fertilized plots ($p > 0.01$). Significant mean direction is obtained only for replicate R1 for the unfertilized plots. No significant mean direction for replicates R2 and R3 of the unfertilized plots means that ramets emergence is distributed uniformly around the circle, that is originating from the mother plant. They occur when s, the dispersion given by the angular deviation is near the maximum

(where $0 < s < 83.01$). Dispersion analysis of ramets by circular statistics on *S. grossus* generated no special preferences in the direction of modules or emerged ramets as explained by the Rayleigh's *r*, Rayleigh's z, and mean angle of dispersion (Table 4.4). However, there were heavier concentrations of ramets in the eastern sector of the plot, presumably due to phototropic effect of sunlight (Fig. 4.28).

Table 4.3 Directional and dispersion statistics on the circular distributions of emerged ramets around the mother plant of *Scirpus grossus* in fertilized (F1) and unfertilized peat soil (F0) as measured by selected attributes

Parameter of soil		Attributes		
	Replicate	R	Z	R
Fertilized Soils	R1	51.74	6.53	65.12
	R2	58.19	6.65	82.39
	R3	111.75	20.74	75.57
Unfertilized soils	R1	78.36	10.89	88.08
	R2	15.86	0.78	*
	R3	21.23	0.86	*

*No mean angle, Raleigh z test showed that ramet emergence is distributed uniformly around the circle

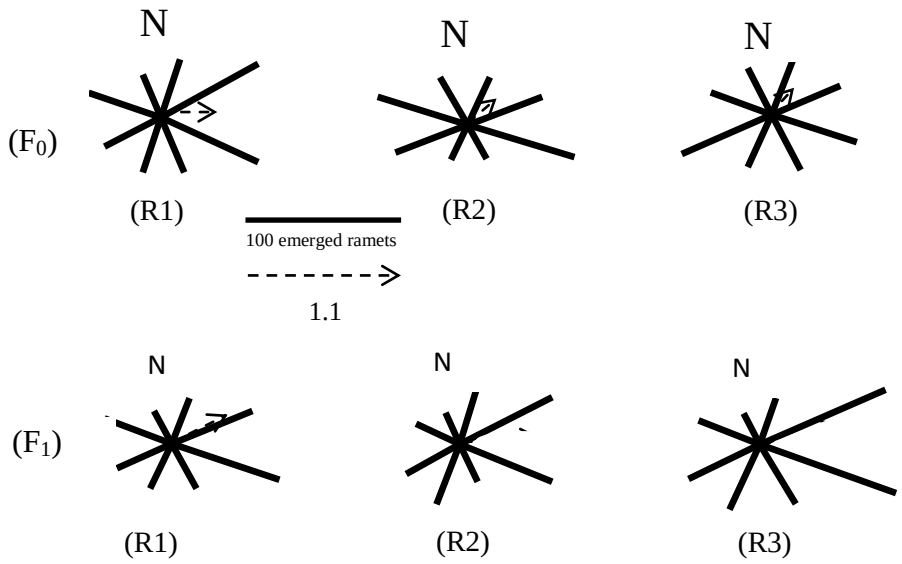

Fig. 4.27 Dispersion analysis of emerged ramets of *Scirpus. grossus* by circular statistics in peat soil with no fertilizer (F0) and soil with fertilizer (F1). N, geographical north; mean angle of dispersion.

Table 4.4 Directional and dispersion statistics on the circular distributions of emerged ramets around the mother plant of *Scirpus grossus* in fertilized (F1) and unfertilized paddy soil (F0) as measured by selected attributes

Parameter of soil	Attributes			
	Replicate	R	Z	θ^o
Fertilized Soils	R1	76.04	15.0	262.79
	R2	28.61	1.61	*
	R3	25.72	2.16	*
Unfertilized soils	R1	137.44	37.26	31.08
	R2	25.23	1.71	*
	R3	31.74	8.13	214.38

*No mean angle, Raleigh z test showed that ramet emergence is distributed uniformly around the circle

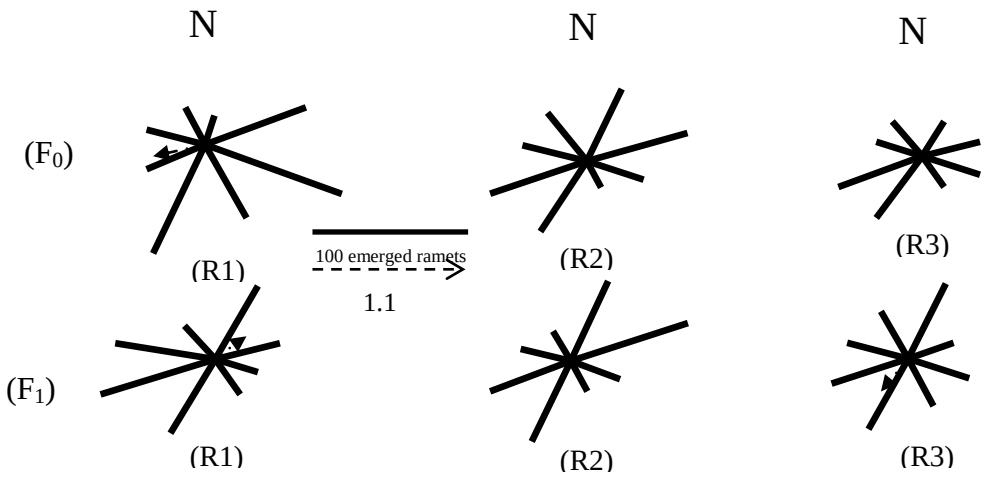

Fig. 4.28 Dispersion analysis of emerged ramets of *Scirpus grossus* by circular statistics in paddy soil with no fertilizer (F0) and soil with fertilizer (F1). N, geographical north; → mean angle of dispersion.

4.3.4 Response surface analyses of *Scirpus grossus* ramets

4.3.4.1 Response surface analyses of *Scirpus grossus* ramets grown in both fertilized and unfertilized peat and paddy soils

The response surface function obtained for the unfertilized plot was;

Density = -19.17 + 0.03 xdis + 4.70 ydis + 40.26 time– 6.20 xdis X ydis

+ 0.25 xdis X time - 0.97 ydis X time - 45.11 $xdis^2$ - 43.0 $ydis^2$

- 2.06 $time^2$ (R^2 = 60.6 %)

For the fertilized plot the function obtained was;

Density = -19.03 + 4.34 xdis + 4.53 ydis + 42.36 time – 16.47 xdis X ydis

+ 0.22 xdis X time - 6.38 ydis X time – 52.06 $xdis^2$ - 43.06 $ydis^2$

- 2.11 $time^2$ (R^2 = 54.2 %)

A significant fit was obtained for the two cases.

Table 4.5 shows the stationary points obtained for the unfertilized plots was at x-distance = 0.03 m, y-distance = - 0.06 m and time = 9.8 months. This function predicted a maximum density of 178 plants m^{-2} to occur at the location and time. For the fertilized plot, the stationary point was at x-distance = 0.20 m, y-distance = - 0.82 m and time = 11.31 months. The predicted density obtained was 291.02 plants m^{-2}.

Table 4.5 indicates that the response surface analyses on plant density at (x-distance, y-distance and time) of *S. grossus* showed the best location and time in unfertilized and fertilized soils. The best location and time in unfertilized soil was between x-distance = 0.04 m and y-distance = -0.08 m at time = 2.52 month, while in fertilized soil the location was between x-distance = 0.26 m and y-distance = -1.10 m and the best time was at time = 3.12 month. Table 4.3 also displays that the maximum *predicted* value at stationary point in unfertilized peat soil was 178.07 at 9.8 month, while in fertilized peat soil it was 219.09 at 11.3 month.

Using the fitted function, a two dimensional contour of density was plotted with x-distance and y-distance as axis, at each monthly time period. Looking at the contours for each time period, a higher density concentrated around the stationary point and it decreased further away from that point. The density increases each month. The pattern of the density contour is the same for both the unfertilized and fertilized plot.

The predicted response surface function on density fitted for the unfertilized plot, F0, was

Density = 29.0 - 0.03 xdis – 11.03 ydis + 3.70 time + 0.85 xdis X ydis

-0.52 xdis X time + 5.89 ydis X time – 61.56 $xdis^2$ – 56.89 $ydis^2$

+ 1.76 $time^2$ (R^2 = 51.07 %)

A reasonably good fit (R^2 = 51 %) was obtained with lack of fit found to be not significantly different for $p < 9\%$, where p is the percentage level of significance tested.

The stationary point obtained for the fitted surface was at x-distance = 0 m, y-distance = -0.14 m and time = 8.16 months. This function predicted a density of 28 plants per m^2 to occur at the stationary point.

Results of canonical analysis, indicated that the predicted response surface was shaped like a saddle. Because the canonical analysis resulted in a saddle point, the estimated surface does not have a unique optimum.

However, results of ridge analysis, indicated that maximum density increased with time and location (x-distance and y-distance). The direction of density changes followed northeast from the mother plant during the 3.5 to 6 months period.

For the fertilized plot, F1, the predicted response function on density obtained was

Density = 34.93 - 3.82 xdis + 2.80 ydis + 14.41 time – 7.31 xdis X ydis

+3.04 xdis X time -2.62 ydis X time – 109.89 $xdis^2$ – 61.0 $ydis^2$

+ 0.80 $time^2$ (R^2 = 62.59 %)

This function, however, has a significant lack of fit for p > 0.01%.

The stationary point obtained for the fitted surface was at x-distance = -0.13 m, y-distance = 0.20 m and time = 8.48 months. Canonical analysis, (Table 4.6) showed that the response surface analyses on plant density at (x-distance, y-distance and time) of *S. grossus* showed the best location and time in unfertilized and fertilized paddy soils. The best location and time in unfertilized soil was between x-distance = 0.00 m and y-distance = -0.14 m at time = 8.16 month, while in fertilized soil the location was between x-distance = -0.13 m and y-distance = 0.20 and the best time at time = 8.48 month.

However, results of ridge analysis,, indicated that maximum density increased with time and location (x-distance and y-distance). The direction of density changes followed southwest from the mother plant during 3.5 to 6 months period.

Table 4.5 Stationary point of fitted response surface on plant density (at x-distance, y-distance and time) of *Scirpus grossus* in peat soil with no fertilizer (F0) and soil with added fertilizer (F1) based on RSREG procedure canonical analysis of response surface based on coded data

	Critical Values	
Factor	F_0*	F_1**
x-dist	0.042206	0.26151
y-dist	-0.077296	-1.097468
Time	2.521772	3.123147
Predicted value at stationary point	178.074472 /9.8	219.018688 /11.3

*F0: The critical values in unfertilized plots.
**F1: The critical values in fertilized plots.

Table 4.6 Results of canonical analysis on the fitted response surface function using RSREG procedure showing stationary point coordinates, predicted density and type of stationary point obtained for *Scirpus grossus* in unfertilized paddy soil (F0) and fertilized paddy soil (F1) based on RSREG procedure canonical analysis of response surface based on coded data

	Critical Values	
Factor	F_0*	F_1**
Xdist	0.002215	-0.128095
Ydist	-0.139144	0.197405
Time	8.15614	8.479282
Predicted density value at stationary point	28.257389	-25.636676
Type of stationary point	Saddle point	Saddle point

*F0: The critical values in unfertilized plots.
**F1: The critical values in fertilized plots.

4.3.5 Plant topography- fractal analyses of ramets

4.3.5.1 Plant topography- fractal analyses of ramets in both fertilized and unfertilized peat and paddy soils

The gray image was divided into a grid of square sub-images, or "boxes", of fixed length, *d*, and the number of boxes containing part of an edge. The results showed values of fractal dimension from gl = 0 to gl = 100 between area-covering and ranched network (1< D > 2). The area-covering concentrated at gl = 0 and gl = 40 in fertilized and unfertilized soils. While after gl = 100 – gl = 255 sporadic distribution (D- 0) in fertilized and unfertilized soils.(Fig. 4.30).

The edge image was divided into a grid of square subimages, or "boxes", of fixed length, *d*, and the number of boxes containing part of an edge. The results show value fractal dimension from gl = 0 – gl = 100 between area-covering and ranched network (1< D > 2). The area-covering concentrated at gl = 0 and gl = 40 in fertilized and unfertilized soils. While after gl = 100 to gl = 255 there was sporadic distribution (D - 0) in unfertilized soils. While in fertilized paddy soil after gl = 100 to gl = 255 founded in ranched network (D -1) (Fig. 4.31).

Significant differences in N concentration by fall fertilization for root, but not for the shoot, indicate that N uptake and storage in roots respond to different concentrations of N in the growing media, but N translocation to shoots is almost null as no differences were found in N concentration based on treatments (Folk and Grossnickle 2000). While P dynamics: Concentration in roots was significantly affected by fertilizer rate and timing, with the highest concentration values at the maximum fertilizer rate applied in early fall. This indicates that P uptake efficiency is higher at the beginning of fall. With regards to shoot, a significant response to fall fertilization (on

average) occurred, indicating a partial translocation to the shoots of the supplied P in the fall (Folk and Grossnickle 2000).

Therefore, low N and K uptake capacity must be explained mostly by a weak sink demand. N uptake has been shown to be greatly dependent upon ontogeny (Imsande and Touraine 1994), and low N uptake amounts are expected during hardening (Silla and Escudero 2003). In other experiments, the relationship between fertilization and root growth responded positively (RGRP) is via P concentration in roots, which appeared positively correlated to new root proliferation (Oliet *et al.* 2009b).

In previous studies showed a significant effect of fertilization on the root growth potential; although this effect could not be associated to any nutrient, in particular, mortality after planting showed a significant and negative relationship with root P (Villar-Salvador *et al.* 2004; Molla *et al.* 2006), fewer seedlings died when roots had more P. Our findings agree with those of Villar-Salvador *et al.* (2004).

Higher N levels in spring have also been shown to accelerate bud burst of *Picea abies* L. (Floistad and Kohmann 2004). Bud bursting earlier in spring can be an interesting advantage for seedlings planted under mild Mediterranean conditions, where summer drought occurs at the very beginning of summer. Furthermore, many studies on the impact of NPK fertilizer for long periods, where the results of these studies showed the continued effect of fertilizer on plants and herbs, but in some studies increases their impact. In a study conducted for eight years during which the use of several different tests to improve the quality of NPK fertilizer, where the results showed that fertilizer medal in the low mortality rate and longer survival of plants alive (Oliveira *et al.* 2011). James *et al.* (2010) reported that on the long-term, NPK addition decreased mortality in the giant cane plant (*Arundo donax*) and observed that periodic burning can increase

density and spread of this species. In 2000 – 2002 field experiment was conducted to evaluate the effect of sawdust mulch and NPK 20:10:10 fertilizer rates on weed flora composition and growth in plantain/cocoyam intercrop.

Mulch influenced high composition (81%) of broad leaves/ herbaceous weeds, which were more abundant in mulched plots, while the gramminaceous species (19%) were mostly found in bare plots (Hol 2010). During two years in 2005 -2006 to study the effect of NPK fertilizer on the growth and yield of wheat *Triticum aestivum* There was 137% increase in shoot dry biomass over control to recommended dose of nitrogen-phosphorus-potassium NPK fertilizer. And there was to 96% increase in grain yield over control (Javaid and Shah 2010). Furthermore, in 2006 - 2007, Field's experiments were conducted cropping seasons on an Alfisol (*Oxic Tropuldalf*) at Owo in the forest-savanna transition zone of Nigeria to evaluate the effect of tillage and fertilizer types on soil properties and sweet potato yield *Ipomoea batatas*. The results increase significantly in leaf area, vine length and increased tuber yield 39% (Agbede 2010). In addition, the NPK fertilizer helped to strengthen the plant, and this was observed in the significant increase in the weights of the various plant parts in fertilized soils. Many previous studies have shown that the application NPK fertilizer can effect clonal growth of crop plants, such as wheat (Ognjanovic *et al.* 1994; Biberdzic *et al.* 2011).

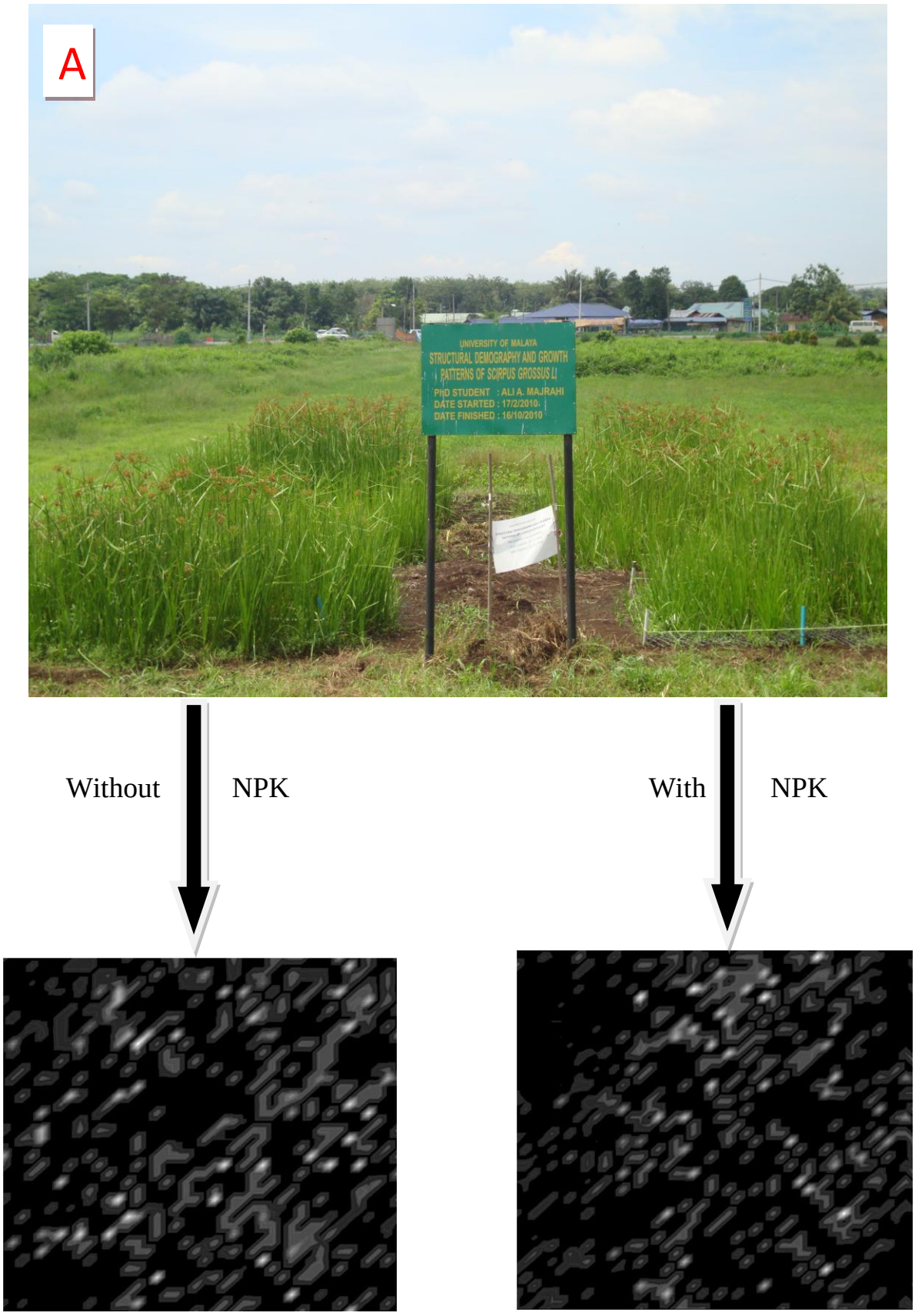

Fig. 4.29a Gray-image for fertilizer and unfertilized peat soil in MARDI Research Station, Jalan Kebun, Selangor, Malaysia.

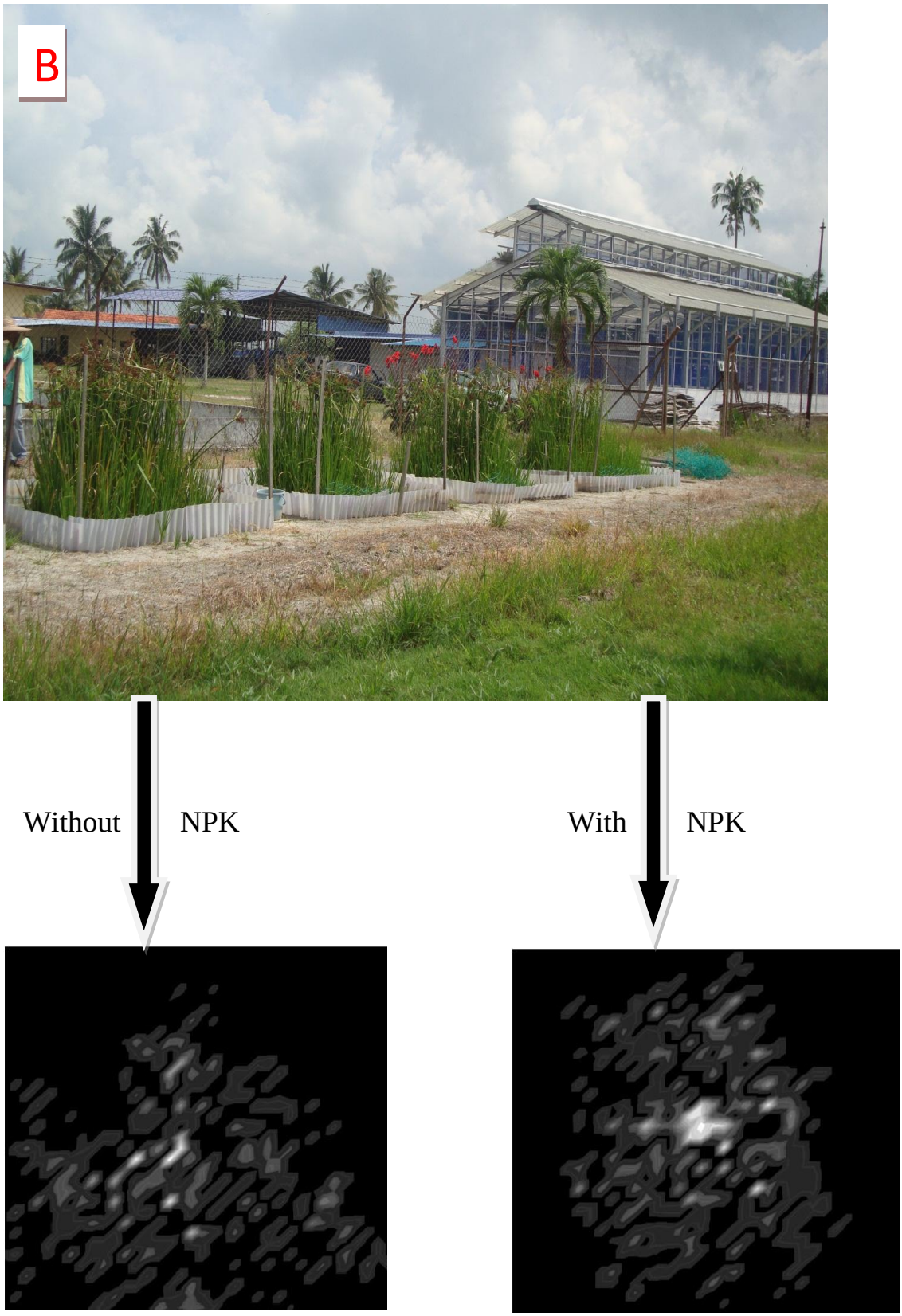

Fig. 4.29b Gray-image for fertilizer and unfertilized paddy soil in MARDI Research Station, Tanjung Karang, Selangor, Malaysia.

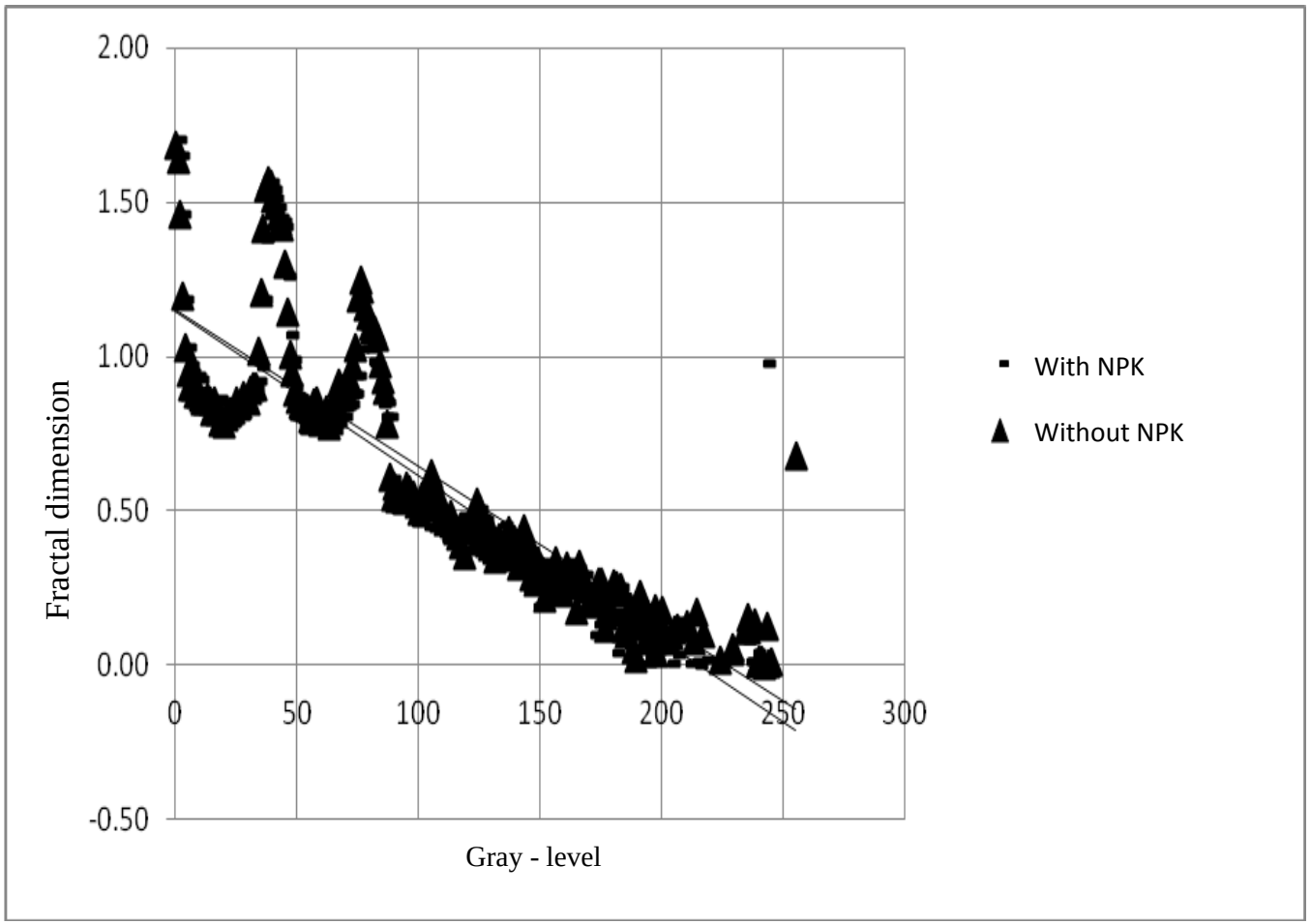

Fig. 4.30 Fractal dimension of gray-level for *S. grossus* grown in fertilized and unfertilized peat soils in MARDI research station, Jalan Kebun, Selangor, Malaysia.

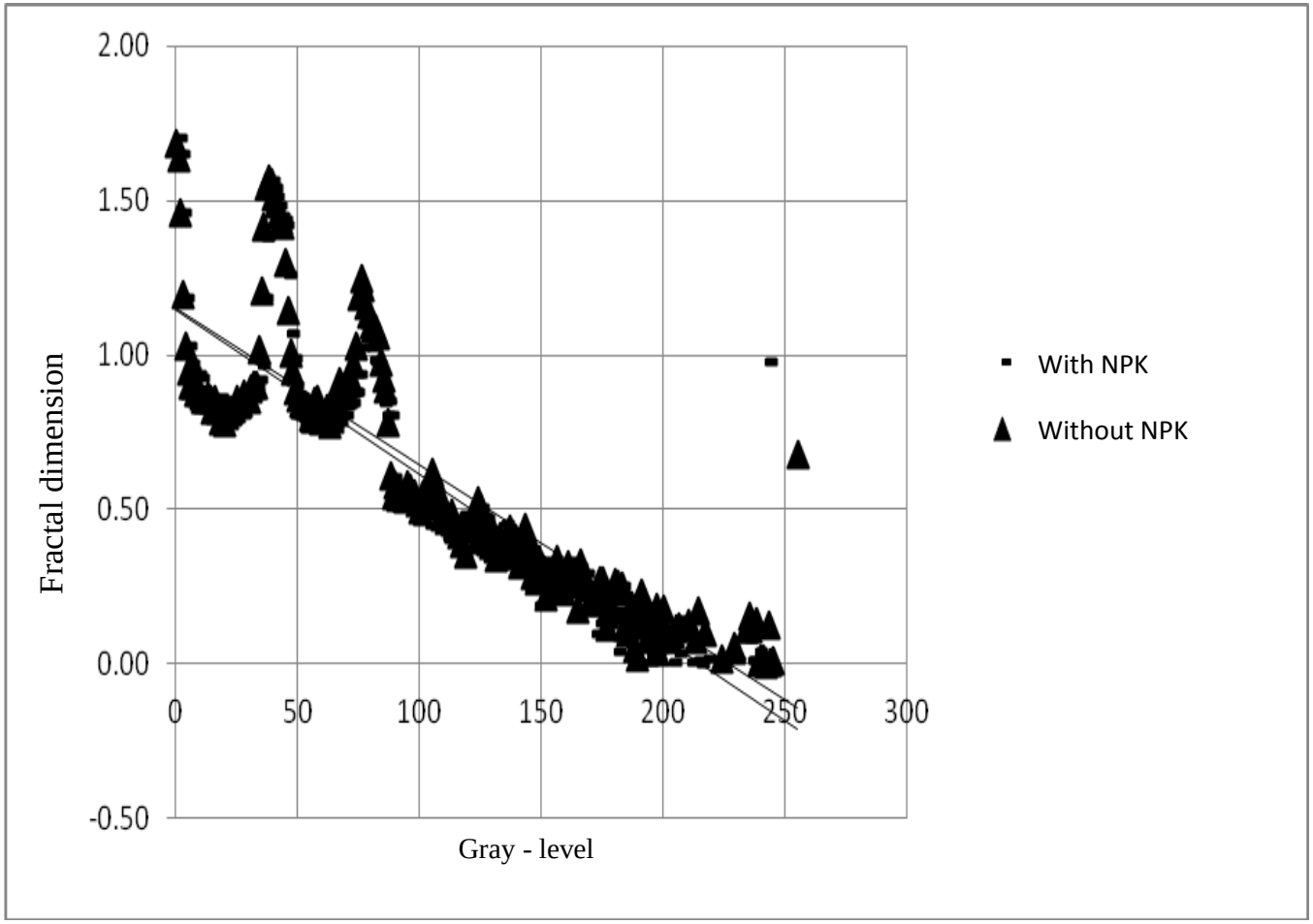

Fig. 4.31 Fractal dimension of gray-level for *Scirpus grossus* grown in fertilized and unfertilized paddy soils in MARDI Research Station, Tanjong Karang, Selangor, Malaysia.